Acknowledgements

It is a pleasure to thank those people who has made this thesis possible. First of all I want to thank my supervisor, Ayumu Tashiro, for the opportunity to work on this project and for good help during the process. This thesis would have been impossible without his great knowledge and experience in neuroscience research.

I also want to show my gratitude to the rest of the colleagues in the Tashiro group for practical help in the lab and for sharing their knowledge with me. A special thanks to the PhD students Stefan Blankvoort and Alessandro Luchetti, who have helped me a lot.

Another thank you goes to the researchers, technicians, administrative personnel, and students at the Kavli Institute for Systems Neuroscience and the Centre for the Biology of Memory for contributing to a great academic and social environment.

Finally, I want to thank my family and friends for their support and encouragement.

Ingrid Åmellem

Trondheim, January 2011

Summary

Neurogenesis occurs in the dentate gyrus of the hippocampus throughout adulthood in a broad range of mammalian species. Several behavioural studies have suggested a role for adult neurogenesis in learning and memory. During maturation the newborn granule cells extend their axons, the mossy fibres, towards the CA3 area in hippocampus, their dendrites towards the molecular layer in dentate gyrus, and are incorporated into existing neural circuits. This process is known to be regulated by neuronal activity and thought to make an important contribution to the function of new neurons in learning and memory. Kainite receptors are located presynaptically on the mossy fibre terminals, and have been shown to be important for the mossy fibre excitatory transmission, synapse formation and synaptic plasticity, and may be involved in maturation of new neurons in the adult dentate gyrus. In this project I aim to understand the mechanism of neuronal maturation mediated by the kainate receptor, and more specifically the kainate receptor subunit GRIK2, which is highly expressed in mossy fibres and has been shown to be necessary for the mossy fibre excitatory currents. The methodological approach in this study is to use retrovirus and RNA interference to block gene expression of GRIK2. As a first step to achieve this, I have established a fluorescence-based screening assay in cell culture, which has been used to test the efficacy of short hairpin RNA (shRNA) sequences for gene silencing. The down-regulation effect of four miRNA-GRIK2 shRNA plasmids has been tested by co-transfecting each of the plasmids with a plasmid containing a mCherry-GRIK2 fusion protein gene. The down regulation of the mCherry-GRIK2 fusion protein was investigated by measuring the fluorescence intensity of the fluorescent protein mCherry. By the use of the screening assay we have identified two shRNA sequences that successfully down-regulated the GRIK2 expression by 90%. The sequences will be further used to establish a role of the kainate receptor in the maturation of adult born dentate granule cells.

Table of contents

1. Introduction

New neurons are generated in the dentate gyrus of the hippocampus throughout adulthood in a broad range of mammalian species (Altman & Das, 1965b). The first report of continuous production of new neurons was made by Altman and Das in the hippocampus of rats over 45 years ago (Altman & Das, 1965b). Neurogenesis has been proved to be a conserved phenomenon, and has been found in different species of rodents (Altman, 1969a; Altman & Das, 1965b; Kaplan & Hinds, 1977) and new and old world primates (Gould et al., 1999; McDermott & Lantos, 1990), including humans (Eriksson et al., 1998). According to Gould and colleagues this suggests that adult neurogenesis is of fundamental biological significance (Gould, Tanapat, Hastings, & Shors, 1999).

1.1 The dentate gyrus

The dentate gyrus is a cortical region connected to a larger functional brain system called hippocampus. The dentate gyrus forms a banana shaped structure, and consists of three layers; the molecular layer, the granule cell layer, and the polymorphic layer also called the hilus (Figure 1) (Amaral, Scharfman, & Lavenex, 2007).

The granule cells are the principal cell type of the dentate gyrus (Figure 2) (Amaral & Witter, 1989). Their cell bodies are about 6-8 µm in diameter and have round or oval nuclei (Seress, 1978). They are tightly packed together and form the granule cell layer, often without a glial sheath interposed between the cells. Granule cells have a cone-shaped tree of spiny apical dendrites, which extend mainly into the molecular layer (Amaral, et al., 2007). The molecular layer is relatively cell body free, and contains the perforant path (PP) axons that originate from the EC layer II (Migliore, 2003), which is a major cortical input into the dentate gyrus (Amaral & Witter, 1989).

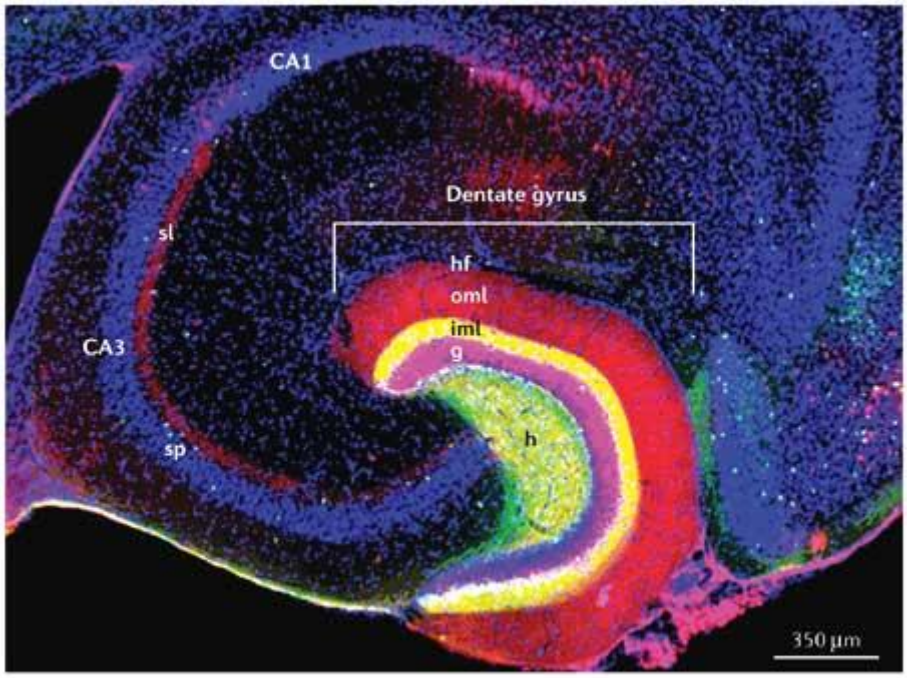

Figure 1. Visualization of the mouse hippocampus, with a particular focus on the dentate gyrus, which is divided into; h (hilus), g (granule cell layer), iml (inner molecular layer), oml (outer molecular layer), and hf (hippocampal fissure). The mossy cells in the hilus are immunostained green for the calcium-binding protein calretinin. The neuronal cell bodies are counterstained for DAPI (blue), which label the pyramidal cell layer (sp) in CA1 and CA3, together with the granule cell layer. The granule cells are also stained for calbindin (red), which is shown in their dendrites that extends towards the molecular layer and their axons, the mossy fibres, that terminates in the stratum lucidium (sl) of CA3 (Forster, Zhao, & Frotscher, 2006).

Each granule cell gives rise to a single axonal fibre, which is called mossy fibre, and form synapses with the CA3 pyramidal cells of the hippocampus, the mossy cells in the hilus, and interneurons in both areas (Amaral & Witter, 1989). The mossy cells in the hilus are characterized by triangular or multipolar shaped somata. They receive input from the granule cells and project back to the granule cells with their axons to the molecular layer (Ribak, Seress, & Amaral, 1985). The interneurons are a morphologically variable group of neurons, many of which use gamma-aminobutyric acid (GABA) as inhibitory neurotransmitter (Houser, 2007).

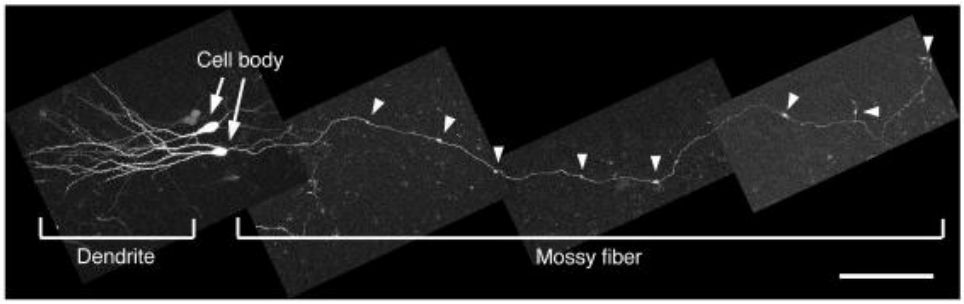

Figure 2. Dentate granule cells in slice culture transfected with green fluorescent protein (GFP). The dendrites, cell bodies and axons (mossy fibres) are clearly visible. The arrowheads are pointing on possible mossy terminals. The scale bar equals 150 µm (Tashiro, Dunaevsky, Blazeski, Mason, & Yuste, 2003).

The mossy fibres have three kinds of terminals; large mossy terminals (4-10 µm in diameter), en passant boutons (0.5-2 µm in diameter), and thin extensions from the mossy terminals called filopodia (0.5-2 µm in diameter) (Figure 3). The large mossy terminals connect to the pyramidal cells in CA3 or the mossy cells in the hilus, while the small filopodia and en passant terminals predominantly connect to inhibitory interneurons secreting GABA. The small filopodial extensions and en passant boutons outnumber the large mossy terminals by approximately 4:1 in CA3 alone and 10:1 when the mossy fibre synapses in the hilus are included (Acsady, Kamondi, Sik, Freund, & Buzsaki, 1998). Several physiological differences have been identified among the three mossy fibre terminals (Lawrence, Grinspan, & McBain, 2004). The large synapses between the mossy fibres and CA3 pyramidal cells have more release sites per synapse (Acsady, et al., 1998), but the small mossy fibre interneuron synapses have a higher probability of transmitter release and a higher efficiency of each release site (Lawrence, et al., 2004). This indicates that activity in the mossy fibre pathway is likely to result in the activation of greater numbers of inhibitory than excitatory cells. The activation of mossy fibres may lead to a net inhibition of the hippocampal CA3 networks (Lawrence, et al., 2004).

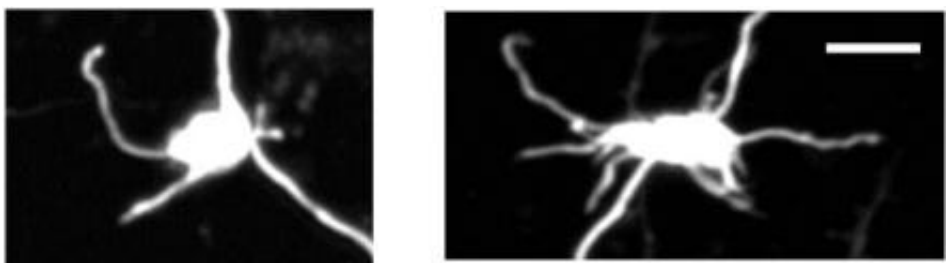

Figure 3. Mossy fibre terminals with filopodial extensions. Scale bar equals 5 µm (Tashiro, et al., 2003).

1.2 The role of hippocampus in learning and memory

There is a lot of evidence suggesting that the hippocampus is involved in formation, processing, storage, and recall of some types of memory (Squire, Stark, & Clark, 2004). The importance of the role of hippocampus in memory was suggested by Scoville and Milner in 1957 from their observations on the patient H.M., who underwent a bilateral hippocampal removal as a treatment for epilepsy. The removal resulted in severe anterograde amnesia, which made H.M. unable to create new episodic memories after the time of the surgery, and also a less severe retrograde amnesia, which made him unable to recall all of the events that occurred before the time of the surgery (Scoville & Milner, 1957).

Animal studies have supported a role of the hippocampus in some forms of learning and memory (Morris, Schenk, Tweedie, & Jarrard, 1990; Moyer, Deyo, & Disterhoft, 1990; Orr & Berger, 1985). Several forms of hippocampal-dependent learning/memory tasks have been used in these studies. For example, in an experiment performed by Morris and colleagues they examined the spatial learning ability of hippocampal lesioned rats by the use of a water maze task in which the rats had to find a hidden platform by using spatial cues (Morris, et al., 1990). They found that a total hippocampal cell loss resulted in a slower rate of place learning and a navigational impairment (Morris, et al., 1990). A trace eye-blink conditioning task was used by Mojer and colleagues to test if the hippocampus plays a role in the learning ability of rabbits with hippocampal lesions (Moyer, et al., 1990). The task aimed that the rabbits should learn an association between a neutral stimulus (a 100 ms tone) and an uncomfortable stimulus (air puff to the eye) when they were separated by a 300 ms or a 500 ms trace interval. All rabbits learned the task with the 300 ms trace interval between the stimuli, but the hippocampal lesioned rabbits did not learn the task when the trace interval was 500 ms (they had only 22% conditioned responses after 25 sessions, whereas the controls showed greater than 80% after 10 sessions) (Moyer, et al., 1990).

The dentate gyrus and the CA3 of the hippocampus have been suggested to have a particularly important role in pattern separation (Leutgeb, Leutgeb, Moser, & Moser, 2007). Pattern separation is the ability of a neural process to create new, independent representations of two similar input patterns more dissimilar, and thereby decreasing the probability of recall errors (I. Lee, Yoganarasimha, Rao, & Knierim, 2004). The capability of spatial pattern separation is required to be able to discriminate between similar environments or objects that are located very close to each other. Gilbert et al. (1998) tested rats with or without hippocampal lesions in spatial separation tasks. They found that the hippocampal

damaged rats were impaired on spatial tasks when there was an increased overlap among distal cues, which presumably increased the spatial similarity. However, the rats performed well when the overlap was minimized, and thereby had less spatial similarity. The results suggest that the hippocampus may serve a function to separate patterns of incoming spatial information by temporarily storing one place from another place. The hippocampal lesions resulted in a decrease in the efficiency in pattern separation that may result in impairment on tasks with increased spatial similarity or interference among spatial working memory representations (Gilbert, Kesner, & DeCoteau, 1998). Gilbert and colleagues further suggested a role for the dentate gyrus in spatial pattern separation (Gilbert, Kesner, & Lee, 2001). They tested rats in a cheese-board maze consisting of a sample phase and a choice phase. During the sample phase the rats entered the maze and displaced an object that covered a baited food-well to receive a food reward. In the choice phase the rats had to choose between two identical objects with a spatial separation of 15-105 cm, which either covered the same re-baited well (correct choice) or an un-baited well (incorrect choice). The dentate gyrus lesioned group performed at chance on 15 cm and 37.5 cm separations between the correct and the incorrect object, but they were able to discriminate objects at 60 cm separation, and matched their preoperative performance at 82.5 cm and 105 cm separations. The improved performance of the rats with increased spatial separation suggests a deficient spatial pattern separation. The CA1 lesioned rats did not show impairment in the task performance, which indicate that spatial pattern separation is a specific role of the dentate gyrus (Gilbert, et al., 2001).

1.3 Adult neurogenesis

New neurons are continuously born throughout adulthood in predominantly two regions of the mammalian brain, the olfactory bulb and the dentate gyrus (Altman, 1969b; Altman & Das, 1965a). Cameron and McKay estimated that about 9000 new cells are produced in the adult dentate gyrus every day, which is about 250 000 new cells a month. This large number of newborn cells indicates that they are important for the function of the hippocampus (Cameron & McKay, 2001). Gould and colleagues showed that the amount of adult neurogenesis in the dentate gyrus is affected by hippocampus-dependent learning tasks (Gould, Tanapat, et al., 1999).

1.3.1 The role of adult neurogenesis in learning and memory

Several studies indicate that the adult born neurons in the dentate gyrus are important contributors to hippocampus-dependent learning and memory (Gould, Beylin, Tanapat,

Reeves, & Shors, 1999; Gould, Tanapat, et al., 1999; Shors et al., 2001; Snyder, Hong, McDonald, & Wojtowicz, 2005). Manipulations that increase neurogenesis in the dentate gyrus, such as voluntary running and housing in an enriched environment, have shown to enhance memory functions in rodents (Kempermann, Kuhn, & Gage, 1997; van Praag, Christie, Sejnowski, & Gage, 1999). Several methods have been used to block neurogenesis to establish a causal relationship between adult neurogenesis and its function, such as low-dose irradiation (Snyder, et al., 2005) and systemic treatment with anti-mitotic drugs (Shors, et al., 2001). Even though the methods have been proved to be effective for inhibition of neurogenesis, their unwanted side effects can lead to data discrepancies (Monje, Mizumatsu, Fike, & Palmer, 2002). Newer approaches that aim to be more specific are viral vectors (Jessberger et al., 2009), RNA interference (RNAi) (Alvarez, Ridenour, & Sabatini, 2006; Jiao et al., 2006), and development of transgenic mouse lines (Deng, Saxe, Gallina, & Gage, 2009; Garcia, Doan, Imura, Bush, & Sofroniew, 2004; Singer et al., 2009).

Irradiation has been shown to reduce proliferation of neuronal progenitor cells by 62% and ablate neurogenesis almost entirely, while sparing the production of other cell types in the adult brain (Monje, et al., 2002). Snyder and colleagues (2005) showed that newborn neurons were eliminated by irradiation while other newborn cell types were not affected. They used a hippocampal-dependent learning task, Morris water maze, to examine the effect of the newborn neurons on the rats' ability to learn and memorize. They did not find a difference in performance between the irradiated and control rats during the task training. To test effects on memory retrieval the rats were tested again after 1, 2 or 4 weeks. After 1 week there were no differences between the groups, but after 2 and 4 weeks the irradiated rats performed significantly worse than the control rats. This indicates that newborn neurons are important for the formation, maintenance or retrieval of long-term spatial memory in rats (Snyder, et al., 2005). Similar results were obtained by Deng and colleagues, which developed a Nestin-tk transgenic mice line, where the herpes simplex virus-thymidine kinase (HSV-tk) gene was specifically expressed in neuronal progenitors in the adult brain from the Nestin promoter/enhancer. Administration of the nucleotide analogue Ganciclovir ablated the dividing tk-expressing progenitor cells, leading to blockade of adult neurogenesis. They found that the mice with ablated neurogenesis had deficits in long-term memory retention in the Morris water maze and their abilities to form both spatial preference and context-evoked fear were impaired. They concluded that the adult born dentate granule cells make a significant contribution to learning and memory at an immature stage of development (Deng, et al., 2009).

One of the proposed mechanisms for memory formation is synaptic plasticity, which refers to any lasting up- or down-regulation of synaptic strength (Martin & Morris, 2002). A long-standing theory of memory formation, which is called the synaptic plasticity and memory hypothesis, may be read like this “activity-dependent synaptic plasticity is induced at appropriate synapses during memory formation, and is both necessary and sufficient for the information storage underlying the type of memory mediated by the brain area in which that plasticity is observed” (Martin & Morris, 2002). One of several types of synaptic plasticity is long-term potentiation (LTP). LTP can be induced by brief high-frequency stimulation of a neural pathway, which results in a long-lasting increase in synaptic efficiency (Bliss & Lomo, 1973). Newborn neurons produce a type of LTP with different characteristics than the type of LTP produced by mature neurons. The young neurons have a relatively low threshold for induction of LTP and also a longer decay time compared to mature neuron LTP. The newborn neuron LTP shows a steady magnitude from the time of induction, while mature neuron LTP gradually declines (Figure 4) (Snyder, Kee, & Wojtowicz, 2001).

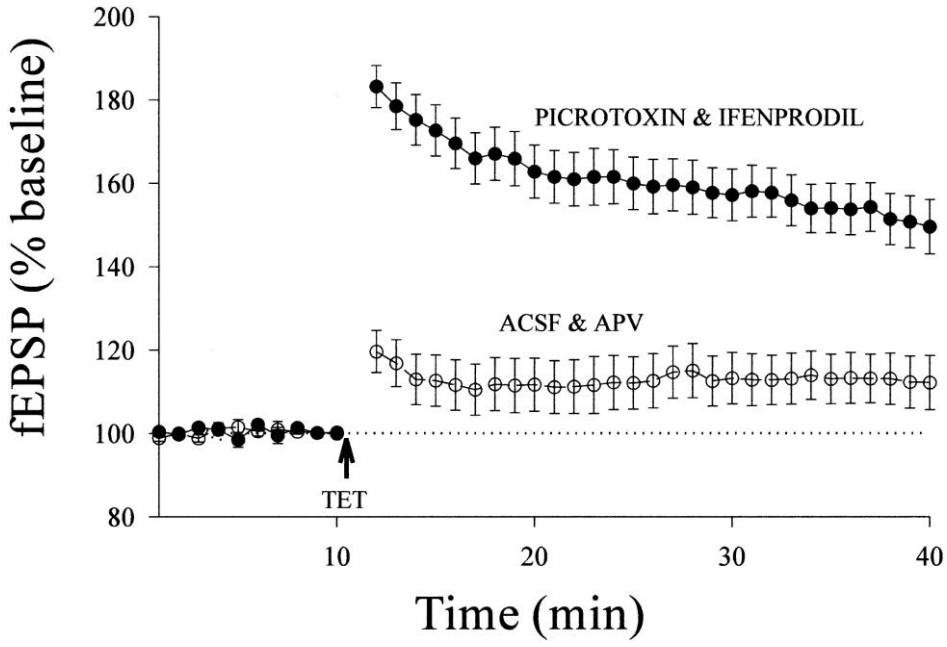

Figure 4. Young granule cell LTP (ACSF & APV) was induced in presence of ACSF (artificial cerebrospinal fluid) and APV (D,L-2-amino-5-phosphonovaleric acid, a NMDA receptor blocker) and showed a steady magnitude from the time of induction. The mature granule cell LTP (picrotoxin & ifenprodil) was induced in the presence of picrotoxin (a GABA receptor blocker) and ifenprodil (blocker of the NR2B subtype of NMDA receptors). It showed a strong post-tetanic potentiation and a gradually declining LTP. A standard tetanic protocol (TET) was used to induce LTP, and it was measured by fEPSP (field excitatory postsynaptic potential) recordings (Snyder, et al., 2001).

The enhanced synaptic plasticity provided by the addition of new neurons might make it more easily for animals to acquire and retain new information. The mature neurons may

contribute to acquisition and short time retention of spatial memory, but they may lack the ability of long-term storage since they have a higher threshold for information storage and limited capacity to keep information over time (Snyder, et al., 2005). However, it has been difficult to formulate basic principles regarding the function of adult neurogenesis in learning and memory so far because of inconsistent results in different animal studies, but future experiments may resolve this question (Deng, Aimone, & Gage, 2010).

1.4 Maturation of adult born neurons

The newborn granule cells originate from undifferentiated precursor cells, which are capable of proliferation and differentiation into both neurons and glia (Cameron, Woolley, McEwen, & Gould, 1993). The precursor cells are located in the subgranular zone between the hilus and the granule cell layer (Kaplan & Hinds, 1977). It is still unclear whether the adult born neurons originate from a resident stem cell population, which has unlimited self-renewal capacity, or from cells with a limited capacity of self-renewal (Bull & Bartlett, 2005).

The morphological maturation of the newborn cells in the dentate gyrus was studied by Zhao and colleagues (Figure 5) (Zhao, Teng, Summers, Ming, & Gage, 2006). They used retroviral vectors to label newborn cells with GFP. Soon after birth, newborn cells started to polarize and migrate to the granule cell layer from the subgranular layer. After three days most of the GFP+ cells were observed at the hilar border of the granule cell layer, but a small portion of cells was located in the middle third and some cells in the outer third of the granule cell layer (Figure 5a). The beginning of the axonal and dendritic growth occurred at the same time as the cells migrated. The apical dendrites reached the inner molecular layer before 10 days after neuronal birth, the middle of the molecular layer at around 14 days and some of the neurons reached the outer edge of the molecular layer before 21 days (Figure 5c). The growth of the axon fibres occurred at the same time as the dendritic growth, and they ended up in the CA3 area. Around the time of the termination of the axonal and dendritic growth, dendritic spines, which receive the majority of excitatory synaptic connections, started to form (Zhao, et al., 2006). Jones and colleagues (2003) got results consistent with this observation in a developing brain. They retrogradely labeled granule neurons with a fluorescent dye, DiI, in fixed sections prepared from 2-9 days old rats. Their data showed that the dendritic outgrowth occurred either before or concurrently with the time the axonal growth reached the CA3 area. The first adult-like granule neurons were observed on postnatal day seven, but they were more common on day nine (Jones, Rahimi, O'Boyle, Diaz, & Claiborne, 2003). Zhao et al. (2006) found a time point for newborn granule neurons when their

morphology started to resemble the typical morphology of mature granule cells at around 10 and 14 days in adult brains, which is later than the time point in developing brains suggested by Jones et al. (2003). Zhao et al. (2006) observed that spine formation started around 16 days after neuronal birth in adult mice brains, while spines where visible already at 12-13 days in neurons marked in 10 days old mice, which indicate a delay of about four days for spine formation in newborn neurons in adult mice brains (Zhao, et al., 2006). Overstreet-Wadiche and colleagues compared the development of newborn granule cells in adults with their development in neonates (Overstreet-Wadiche, Bensen, & Westbrook, 2006). To identify newborn granule cells they used transgenic mice expressing EGFP (Enhanced GFP) under the control of the pro-opiomelanocortin promoter. The EGFP-labeled granule cells had indistinguishable immature neural morphology and electrophysiological properties in both the adult and neonatal mice, which indicate that they were in the same functional stage. However, the morphological maturation was slower in granule cells born in adult mice compared to the granule cells born in neonatal mice (Overstreet-Wadiche, et al., 2006).

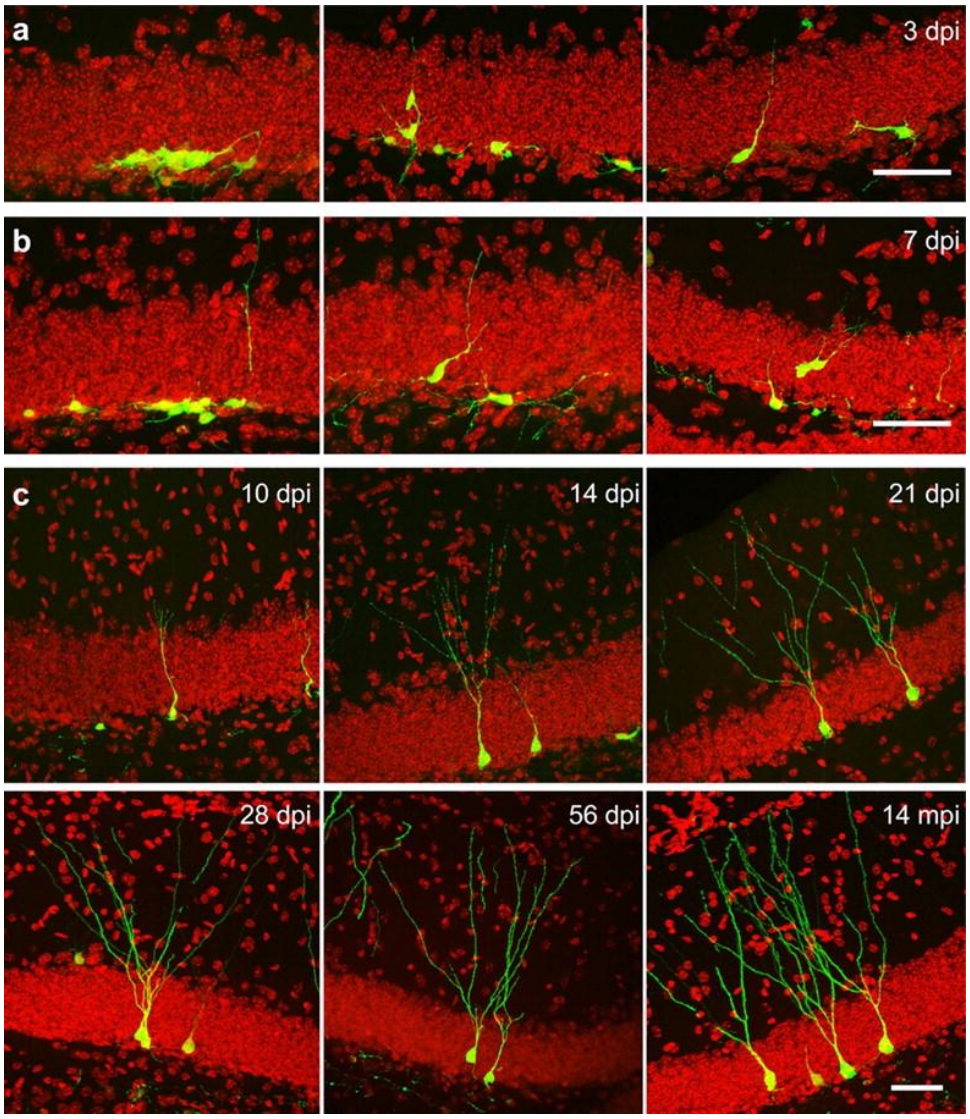

Figure 5. Retrovirus mediated GFP-labeling of newborn neurons showed the morphological development in adult mice brains. Mice were killed at the time points indicated at each picture; a) 3 dpi (days post injection), b) 7 dpi, and c) 10 dpi, 14 dpi, 21 dpi, 28 dpi, 56 dpi, and 14 mpi (months post injection). The molecular layer is oriented upwards. The scale bars are 50 µm. The red color in the pictures is DAPI staining and the green is GFP (Zhao, et al., 2006).

1.5 Activity-dependent maturation of newborn neurons

The morphological maturation described in the previous paragraph is affected by learning and neural activity. In the study by Overstreet-Wadiche et al. (2006) they suggest that activity-dependent processes are involved in the development of newborn granule cells by influencing the maturation, as well as the proliferation and differentiation of newborn neurons. They imply that the higher neural activity in neonatal mice brains compared to adult mice brains may promote faster maturation of the newborn cells by the depolarizing GABAergic activity and gene expression in surrounding cells (Overstreet-Wadiche, et al., 2006). In support of a contribution by activity-dependent factors on maturation, they also found a

reduced rate of neuronal maturation in neonatal mice with reduced network activity due to genetic deletion of the GABA synthetic enzyme glutamic acid decarboxsylase 65. These results support the idea that neural activity around newborn granule cells is an important regulator of maturation (Overstreet-Wadiche, et al., 2006). Ge and colleagues also suggested a mechanism for activity-dependent regulation of adult neurogenesis, in which the newborn neurons may sense neural network activity through the neurotransmitter GABA (Ge et al., 2006).

Tashiro and colleagues found that one week of exposure to an enriched environment around the second week after neuronal birth increases the survival of newborn neurons and also the number of newborn neurons activated by re-exposure to the same environment (Tashiro, Makino, & Gage, 2007). The expression of the immediate early gene products, c-fos and Zif268, were used as indicators of recent neuronal activation. The same measurements were not observed during the fourth week or in a long-time exposure after four weeks, which indicate a critical time period for these effects during the first three weeks after birth of the neurons (Tashiro, et al., 2007). The results showed that a previous experience led to an experience-specific increase in the number of activated newborn neurons, which suggests a possible experience-dependent mechanism for the contribution of newborn neurons in learning and memory (Tashiro, et al., 2007). In another study, Tronel and colleagues used doublecortin staining and retroviral labeling to examine whether spatial learning in the water maze affected the morphology of adult born neurons (Tronel et al., 2010). They found that spatial learning not only affected the number of newborn neurons, but also accelerated their maturation and increased the complexity of dendritic arbors. The studies above suggest that there is an activity-dependent mechanism for the regulation of newborn granule cell maturation. We are interested in finding out how the maturation of new neurons is regulated and how such regulation of maturation is involved in the function of newborn neurons in learning and memory.

1.6 Functions of kainate receptors in mossy fibres

The ionotropic glutamate receptors are classified into NMDA (*N*-methyl-D-aspertate), AMPA (α-amino-3-hydroxy-5-methyl-isoxazole-4-propionate) and kainate (KA) receptors (Egebjerg, Bettler, Hermans-Borgmeyer, & Heinemann, 1991). The KA receptors are ligand-gated channels that are permeable to cations and they are activated by the neurotransmitter glutamate and the agonist kainate. KA receptors consists of the subunits GRIK1/GluR5 (Sommer et al., 1992), GRIK2/GluR6 (Egebjerg, et al., 1991), GRIK3/GluR7 (Schiffer,

Swanson, & Heinemann, 1997), GRIK4/KA1 (Werner, Voigt, Keinanen, Wisden, & Seeburg, 1991), and GRIK5/KA2 (Herb et al., 1992). The GRIK1-3 subunits are capable of making functional homomeric channels, while the GRIK4 and 5 subunits only can make functional heteromeric channels (Chittajallu, Braithwaite, Clarke, & Henley, 1999). KA receptors have been localized to both postsynaptic and presynaptic membranes, and the presence of high-affinity binding sites for kainate on mossy fibres have been known for a long time (Schmitz, Mellor, Frerking, & Nicoll, 2001). Monaghan and Cotman used autoradiography carried out with [^{3}H]kainate to show that the presence of high-affinity kainate binding was restricted to stratum lucidum in the hippocampus, which is the termination zone for mossy fibres (Figure 6) (Monaghan & Cotman, 1982). Represa and colleagues found a more precise localization of these high-affinity binding sites on the presynaptic mossy fibres by a significant reduction of high affinity [^{3}H]kainate binding in stratum lucidum after a selective destruction of mossy fibres, which was not observed after a selective destruction of CA3/CA4 pyramidal cells (Represa, Tremblay, & Ben-Ari, 1987).

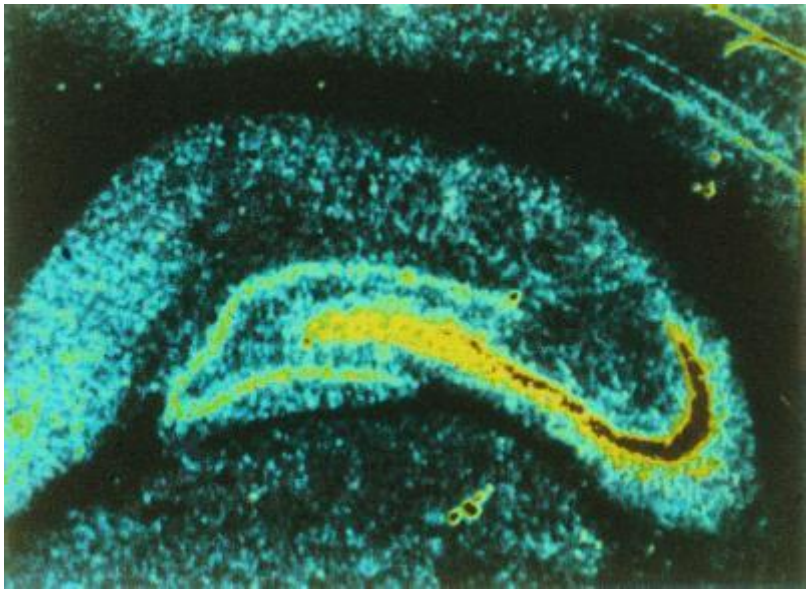

Figure 6. A coronal section of the hippocampus, which shows the distribution of high density kainate binding sites localized to the stratum lucidum, which is the termination zone for mossy fibres. The binding site density is colour-coded with high to low densities represented by red-yellow-blue. Copyright 1982, Elsevier Science, taken from (Schmitz, Mellor, Frerking, et al., 2001).

The KA receptors on mossy fibres have been shown to be important for excitatory postsynaptic currents in CA3 pyramidal cells. Castillo and colleagues applied repetitive stimuli to the mossy fibre pathway in the presence of an AMPA receptor antagonist, and discovered a slow excitatory synaptic current which was antagonized by an AMPA/kainate

receptor antagonist. They concluded that the KA receptors had to be responsible for the observed excitatory synaptic current (Castillo, Malenka, & Nicoll, 1997). Another function of the KA receptors is their important role in regulation of short-term plasticity. Schmitz and colleagues found that synaptically released glutamate can act heterosynaptically on presynaptic KA receptors, which functions as facilitatory autoreceptors. That implies that the short-term plasticity of the mossy fibre-CA3 synapses is partly mediated by the long-lasting activation of a kainate receptor (Schmitz, Mellor, & Nicoll, 2001). Schmitz et al. (2001) also showed that low concentrations of kainate (>50 mM) enhanced neurotransmitter release, while high concentrations inhibited release. On the basis of the bidirectional action of kainate, it might be the amount of synaptically released glutamate that determines whether a facilitation or inhibition is generated by KA receptors (Schmitz, Mellor, & Nicoll, 2001). Schmitz and colleagues later found that even though KA receptors are not required for mossy fibre LTP, the threshold for inducing LTP is strongly dependent on the activation of presynaptic KA receptors (Schmitz, Mellor, Breustedt, & Nicoll, 2003).

KA receptors have also been shown to be involved in the regulation of axonal filopodial growth during development. The filopodial growth is rapid during development, but it slows down as the filopodia move closer to its targets, which indicate that filopodia are involved in the search for its postsynaptic target and slows down when it is found (Tashiro, et al., 2003). Tashiro and colleagues showed that long-term blockage of KA receptors in developing hippocampal slices prevented the normal developmental decrease in the motility of the axonal filopodia, which indicates a regulating function of KA receptors (Tashiro, et al., 2003). They suggested that the effect of neuronal activity on the motility of filopodia could be a dual regulation by glutamate. A stimulatory effect occurs when the axonal filopodia needs help to find its synaptic target, and an inhibitory effect is induced when synaptic connection has been made. This indicates that different levels of neuronal activity can produce growth or retraction of axons and dendrites (Tashiro, et al., 2003). The important roles of KA receptors in the regulation of several different functions of granule cells makes us wonder whether the kainate receptor is involved in the maturation of mossy fiber/mossy fiber terminals, the maturation of newborn neurons in general, or just in the adult brain. We therefore decided to study the KA receptor in this experiment.

The four KA receptor subunits GRIK2, 3, 4, and 5 are highly expressed in dentate granule cells (Schmitz, Mellor, Frerking, et al., 2001), while it has been reported low expression of the GRIK1 subunit (Wisden & Seeburg, 1993). Several studies have reported an absence of KA

receptor-mediated excitatory postsynaptic currents in the CA3 region of GRIK2 knockout mice (Contractor, Swanson, Sailer, O'Gorman, & Heinemann, 2000; Mulle et al., 1998). Based on these observations it seems likely that the presynaptic KA receptors on dentate granule cells contain GRIK2, and we therefore decided to make it the target in this study.

1.7 The purpose of this project

The ultimate goal in this project is to establish a role for the kainate receptor in the maturation of adult born dentate granule cells. In this thesis project, for the first step towards this goal, we have aimed to identify short hairpin RNA sequences for successful RNA interference of the kainate receptor subunit GRIK2 gene expression.

2. Methodology

2.1 RNA interference

RNA interference (RNAi) is a phenomenon where double-stranded RNA (dsRNA) inhibits the expression of mRNA and thereby leads to gene silencing (Fire et al., 1998). Fire and colleagues discovered that injection of dsRNA with sequences corresponding to a given mRNA gave gene silencing specific for the mRNA. They showed that dsRNA injection is more effective compared to single-stranded RNA injection, which had been known for many years (Fire, et al., 1998). RNAi is a taxonomic conserved phenomenon that has been observed in plants (Cogoni, Romano, & Macino, 1994; Napoli, Lemieux, & Jorgensen, 1990), fungi (Cogoni & Macino, 1997; Romano & Macino, 1992) and animals (Fire, et al., 1998). MicroRNA (miRNA) is among the non-coding RNAs expressed in the cell, and is involved in post-transcriptional gene regulation (Ambros, 2001). The short interfering RNAs (siRNAs) that guides the RNAi functions very much like miRNAs in mechanisms for gene silencing, but have some differences in the maturation processes (Du & Zamore, 2005).

The primary miRNA transcript is processed by the RNase III enzyme Drosha to create a ~70 nucleotides long hairpin structure (Y. Lee et al., 2003). The hairpin is cut by the RNase III family nuclease Dicer into 21-23 nucleotides long miRNAs/siRNAs and initiates the miRNA/RNAi process (Bernstein, Caudy, Hammond, & Hannon, 2001). The miRNA/siRNA is incorporated into an enzyme complex called RNA-induced silencing complex (RISC), which target the complementary mRNA molecule (Hammond, Bernstein, Beach, & Hannon, 2000). The miRNA/siRNA-RISC complex either marks the mRNA molecule for degradation or inhibits the mRNA from being translated into protein, depending on how perfectly the molecules match the target mRNA (Zeng, Wagner, & Cullen, 2002).

The application of RNAi can be performed through two types of molecules, the chemically synthesized ds siRNA or vector based short hairpin RNA (shRNA) (Yu, DeRuiter, & Turner, 2002). shRNAs are synthesized in the nucleus of cells where both strands of a siRNA duplex are included in a single RNA molecule separated by a loop. It is further processed and translocated to the cytoplasm, and then incorporated into the RISC activity. A strategy used in the DNA vector-based RNAi systems is RNA polymerase III promoter driven transcription, which enables the endogenous production of the RNA transcripts. The small nuclear RNA U6 (U6) and RNase P RNA H1 (H1) promoters from human and mouse have been frequently

used (Wu et al., 2005). In this thesis we have used a method where the shRNAs are designed to be processed similarly to the miRNA maturation pathway. The shRNAs are synthesized by the use of an expression vector, and like miRNAs it is transcribed by RNA polymerase II (Cullen, 2005).

2.2 Design of shRNA screening

We decided to use the Pol II miR RNAi Expression Vector system from Invitrogen (Carlsbad/CA, USA)[1] to do the RNAi analyses of the GRIK2 gene because this is compatible with the RV-CAG retroviral vector, which has been extensively used for genetic manipulation of newly born neurons in our lab. The Pol II-based system utilizes the expression of shRNA from the expression vector pcDNA6.2-gw-EmGFP-miRNA (Figure 7). The system provide a Gateway-adapted expression vector, which is a universal cloning method that takes advantage of the site-specific recombination properties of bacteriophage lambda (Landy, 1989) to provide a rapid and efficient way to move the DNA sequence of interest into multiple vector systems. The miRNA genes are transcribed from the CMV (cytomegalovirus) promoter by RNA polymerase II, which is active in most mammalian cells. The vectors permit visual selection of cells expressing the pre-miRNA through co-cistonic expression of the fluorescent protein EmGFP (Emerald GFP), which functions as a reporter gene downstream of the promoter and upstream of the pre-miRNA. Fluorescent proteins emit fluorescence upon excitation. They originate from natural occurring bioluminescent proteins, like GFP isolated from the jellyfish *Aequorea victoria* (Shimomura, Johnson, & Saiga, 1962). EmGFP is a mutant of the original GFP with enhanced brightness.

[1] http://tools.invitrogen.com/content/sfs/manuals/blockit_miRNAexpressionvector_man.pdf

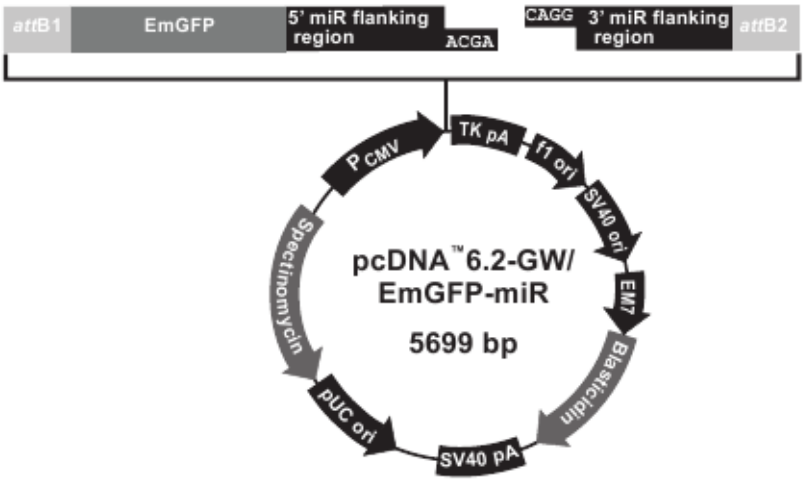

Figure 7. A schematic figure of the expression vector, pcDNA6.2-gw-EmGFP-miRNA, provided by Invitrogen[2].

Single-stranded (ss) oligonucleotides that form shRNA sequences targeting the mouse GRIK2 mRNA (miRNA-GRIK2) were pre-designed and available from Invitrogen's database. The pre-made miRNA sequences are not validated, but are guaranteed to give at least 70% reduction in gene expression by one out of four sequences. The shRNAs are composed of ss oligos encoding the pre-miRNA sequences (top strand oligos) and their complements (bottom strand oligos). The oligos encoding the pre-miRNAs contains five nucleotides derived from the endogenous miR-155 on both ends that is the basis for the miRNA vector system developed in the laboratory of David Turner (Chung et al., 2006). They are specifically designed to allow expression of miRNA sequences, and they also contain a four nucleotide 5' overhang, which is compatible with a four nucleotide overhang in the vector plasmid. The core sequence of the oligo is 21 nucleotides complementary (antisense) to the target mRNA. Two nucleotides from the sense target sequence are removed to create an internal loop, and 19 nucleotides derived from the miR-155 form a terminal loop. The folded hairpin structure of miRNA-lacZ is shown below (the lacZ-miRNA sequence that target lacZ mRNA is shown in red).

```
UG|                UU             UUGGCC
  CUGAAAUCGCUGAU   GUGUAGUCGUU        \
  ||||||||||||||  ||||||||||:         A
  GACUUUAGCGACUA   CACAUCAGCAG       /
AG^                --             UCAGUC
```

[2] http://tools.invitrogen.com/content/sfs/manuals/blockit_miRNAexpressionvector_man.pdf

We constructed plasmids with four different shRNAs against GRIK2 mRNA; pcDNA6.2-gw-EmGFP-miRNA-GRIK2.4, pcDNA6.2-gw-EmGFP-miRNA-GRIK2.5, pcDNA6.2-gw-EmGFP-miRNA-GRIK2.6, and pcDNA6.2-gw-EmGFP-miRNA-GRIK2.7. A plasmid containing the GRIK2 gene fused to the fluorescent protein mCherry (pd-mCherry-GRIK2) was prepared (Figure 8), which made it possible to determine the down-regulation of the GRIK2 gene by measuring the mCherry fluorescence. A control plasmid, pcDNA6.2-gw-EmGFP-miRNA-lacZ, was already available in the lab.

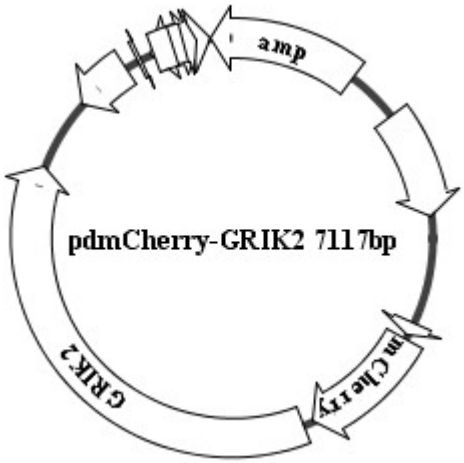

Figure 8. A schematic figure of the pd-mCherry-GRIK2 plasmid.

To investigate the down-regulation effect of the miRNA-GRIK2 plasmids a screening assay was established by co-transfection of each of the miRNA-GRIK2 plasmids and the control miRNA-lacZ plasmid with pd-mCherry-GRIK2. After a few days of incubation the expression of GRIK2 in the co-transfected cells could be investigated by measuring the fluorescent intensity from the fusion protein mCherry-GRIK2. Cell culture was used in this screening because it is much easier than directly use viral vectors and an animal model.

2.3 Materials and procedures

The experimental procedures are presented in the overview bellow. Each step is further explained in a separate section.

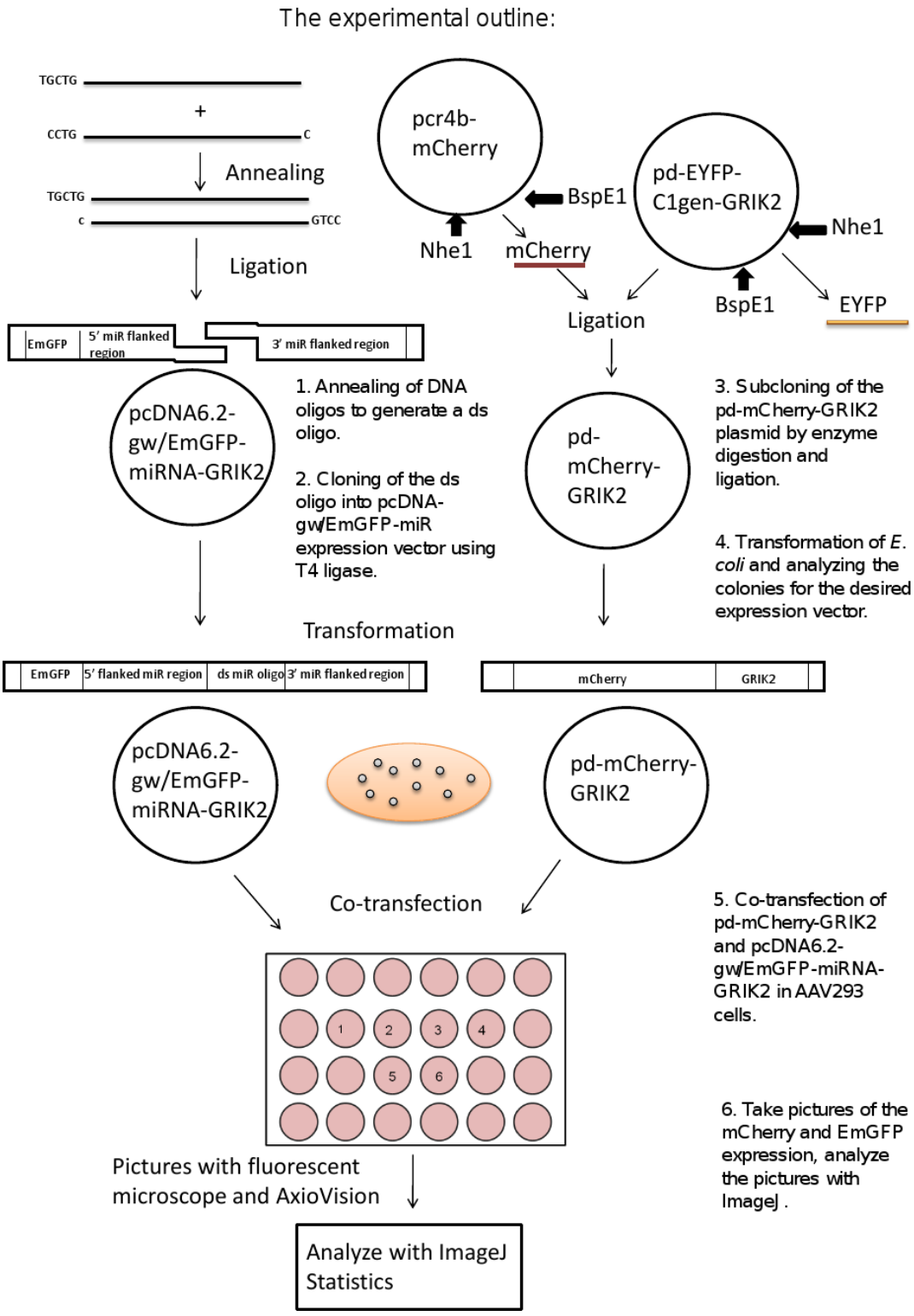

2.3.1 Construction of shRNA plasmids and pd-mCherry-GRIK2

The steps in the construction of the pcDNA6.2-gw-EmGFP-miRNA-GRIK2 plasmids and the pd-mCherry-GRIK2 plasmid are described in the following sections.

Annealing of single-stranded oligos to double-stranded oligo

Eight pre-designed oligos for four different shRNA sequences were ordered from Invitrogen[3]. The pairs of single-stranded oligos were annealed to generate a double-stranded (ds) oligo. The annealing reaction consisted of 200 µM top strand oligo (5 µl), 200 µM bottom strand oligo (5 µl), 10x oligo annealing buffer (2 µl), and DNase/RNase-free water (8 µl). The reaction mixture was heated at 95°C for 4 minutes, and then cooled down in room temperature for 5-10 minutes. The mixture was spun down in a micocentrifuge for 5 seconds and mixed gently. The ds oligos were diluted 5000-fold by performing serial 100-fold and 50-fold dilutions, the first into DNase/RNase-free water and the second into 1x oligo annealing buffer. The final concentration of the ds oligos was 10 nM.

Subcloning of the pd-mCherry-GRIK2 plasmid

The vector plasmid pd-EYFP-C1gen-GRIK2, which was purchased from Source BioScience imaGenes (Berlin, Germany)[4], was digested by the restriction enzymes Nhe1 and BspE1 to cut out the EYFP gene. The mCherry reporter gene was cut out of the plasmid pcr4b-mCherry by the same restriction enzymes, and ligated into the vector plasmid, to form the pd-mCherry-GRIK2 plasmid.

The restriction enzymes, buffers and bovine serum albumin (BSA) were all purchased from New England Biolabs Ltd. (Ipswich/MA, USA, www.neb.com). The buffers and temperature that gave the optimal digestion were selected by using a chart provided by NEB[5]. The two selected enzymes had a different buffer, Nhe1 cleaves 100% in buffer 2 and BSA, and BspE1 cleaves 100% in buffer 3. Therefore, the restriction reaction was first added DNA (8 µg), Nhe1 (1 µl), buffer 2 (2 µl), BSA (0.2 µl) and H_2O to a total of 20 µl. The reaction incubated in 37°C for 1 hour, before BspE1 (1 µl), buffer 3 (2 µl) and H_2O were added to a total of 40 µl. The reaction incubated one more hour in 37°C.

[3] http://tools.invitrogen.com/content/sfs/manuals/blockit_miRNAexpressionvector_man.pdf
[4] http://www.imagenes-bio.de/products/orfclones/shuttle/
[5] http://www.neb.com/nebecomm/tech_reference/restriction_enzymes/buffer_activity_restriction_enzymes.asp

The next step was separation of the DNA fragments by gel electrophoresis. The gel was made by 1% agarose in 100 ml TAE buffer. After the gel had cooled down and hardened for 20 minutes, 10x loading buffer (4 µl) was added to each sample and resuspended before 40 µl was applied to each well. The electrophoresis was performed for about 40 minutes at about 97. The gel was then stained for 30 minutes in a staining bath with ethidium bromide (10 µl) in TAE buffer (200 ml). The DNA bands on the gel were visualized with UV-light and the bands corresponding to the size of the insert and vector were cut out and collected.

The DNA was purified with the Qiagen Qiaquick gel extraction kit (www.qiagen.com), and eluted with 50µl H_2O.

Ligation of the plasmids

The ds oligos were cloned into the pcDNA6.2-gw-EmGFP-miRNA vector (Invitrogen[6]) by ligation. The ligation reaction mix consisted of 5x ligation buffer (4 µl), pcDNA6.2-gw-EmGFP-miRNA (5 ng/µl, linearized (2 µl)), 10 nM ds oligo (4 µl), DNase/RNase-free water (9 µl), and T4 DNA ligase (1 µl). The reaction mix was mixed well and incubated for 5 minutes at room temperature. The pd-mCherry-GRIK2 plasmid was ligated after the protocol Roche rapid DNA ligation kit (www.roche-applied-science.com). The ratio for the oligo insert and plasmid backbone was 3:1.

Transformation

The plasmids were transformed into Top10 chemically competent *E. coli* cells (www.invitrogen.com) after the ligation. 5 µl of the ligation mixture was added to the cells, which were kept on ice for 30 minutes. The cells were then heat shocked in exactly 30 seconds in a 42°C water bath. S.O.C. medium (2% tryptone, 0.5% yeast extract, 10 mM NaCl, 2.5 mM KCl, 10 mM $MgCl_2$, 10 mM $MgSO_4$, 20 mM glucose, www.invitrogen.com) (250 µl) was added to the cells and the tubes incubated in the 37°C shaker for 1 hour. After 1 hour, 20-100 µl of bacterial culture containing the pcDNA6.2-gw-EmGFP-miRNA-GRIK2 plasmids were plated out on pre-warmed LB agar plates with spectinomycin (50 µl/ml). The bacterial culture containing the pd-mCherry-GRIK2 plasmid was plated out on a LB agar plate with ampicillin (50 µl/ml). The plates incubated overnight at 37°C. A few colonies were picked with a pipette tip from each of the plates the next day, and added to separate tubes

[6] http://tools.invitrogen.com/content/sfs/manuals/blockit_miRNAexpressionvector_man.pdf

with growth medium (3 ml growth medium and 6µl spectinomycin/ampicillin in each tube). The tubes were then left in the incubator over night in 37°C with 225 RPM (revolutions per minute).

Miniprep

Miniprep was performed on the pd-mCherry-GRIK2 plasmid according to the protocol QuickLyse Miniprep Handbook (www.qiagen.com). The DNA from the miniprep was used to find out if the cells contained the correct plasmid. The plasmid was digested with the restriction enzyme Nco1. The enzyme digestion reaction contained DNA (5 µl), buffer 4 (4 µl), Nco1 (1 µl), and distilled H_2O (30 µl), and the reaction mixture incubated in a 37°C water bath for 1 hour. The bands were separated with gel electrophoresis to identify the sample with the DNA fragments of the predicted molecular weight.

Growth of colony for maxiprep

A correct sample from each plasmid was used to grow a colony. 100 µl of the bacteria sample was added to 250 ml of growth medium and 1 ml of spectinomycin/ampicillin in an autoclaved marked flask. The flask was then left in the shaker over night (37°C and 225 RPM). Maxiprep was performed the next day to produce a sample of the plasmid with high yield. The protocol: HiSpeed Maxi Kits (www.qiagen.com) was followed. A JA-10 rotor was used on the centrifuge. The density of the DNA was measured with spectrometry. TE buffer (200 µl) was used as a blank sample, and 20 µl of the plasmid was added to measure the density of DNA. An average of several sample measures was used. A new enzyme digestion and separation with gel electrophoresis were performed to check if the maxipreps contained the correct plasmids.

2.3.2 Cell culture

AAV293 cells (www.stratagene.com) were used in this project. The cells are derived from the normal HEK293 (human embryonic kidney) cell line.

Preparation of cell culture

500 ml Dulbecco's Modified Eagle Medium (DMEM) (www.invitrogen.com/GIBCO) with 4.5g/L glucose and L-glutamine was added penicillin streptomycin (5 ml), 10 % FBS, 100x MEM (5 ml), and 100x sodium pyruvate (5 ml). An AAV293 cell stock was taken out of liquid

nitrogen and defrosted in a water bath to start a new cell line. The cells were added to 4 ml of preheated DMEM and centrifuged for 5 minutes with 200*g*. The supernatant was discarded and new 4 ml of DMEM was added. The cells were resuspended gently before medium to a total volume of 10 ml was added. The medium with cells were transferred to a plate and left in a 37°C incubator. The cells had to be passaged every 3rd day.

Procedure for cell passaging

DMEM medium and 0.05% trypsin-EDTA (www.invitrogen.com/GIBCO) were preheated to 37°C. The fluid in the old plate was removed, and the cells were rinsed with 1x Dulbecco's Phosphate Buffered Saline (DPBS) (www.invitrogen.com/GIBCO). 0.05% Trypsin-EDTA (0.5 ml) was added and the cells incubated for 1-2 minutes in 37°C to digest the extracellular matrix around the cells. DMEM medium was added to the cell plate, and the cells were resuspended in the medium to a homogeneous mixture. The medium with cells was added to a tube, and centrifuged at 200*g* for 2-3 minutes. The supernatant was discarded, and new DMEM medium (10 ml) was added. The cells were mixed in the medium to a homogenous mixture by resuspension. The cells were then ready to be transferred onto new plates with fresh DMEM medium and incubated in 37°C.

2.3.3 Transfection of plasmids in cell culture

The down-regulation effect of shRNAs from the pcDNA6.2-gw-EmGFP-miRNA-GRIK2 plasmids on the GRIK2 mRNA was checked by looking at mCherry reporter gene expression from the pd-mCherry-GRIK2 plasmid in the co-transfected cell culture. 1.5-2.0x10^5 AAV293 cells were added to DMEM medium (1 ml) in six wells in a 24-well plate 24-48 hours before transfection. Counting of cells was done by mixing 10 µl of cells in medium suspension, 40 µl DMEM medium and 50 µl tryptophan blue in a 1.5 ml tube. 10 µl of the mixture was pipetted on to the counting frame between the microscope slide and the cover chip. Cells were counted in each of the four big squares, and the average number was calculated. The dilution of cells in medium gave the volume: counted cell number x 10^5 cells/ml in the cell suspension.

Transfection was performed when the cells were 50-70% confluent. 0.4 µg of the plasmid pd-mCherry-GRIK2 was co-transfected with 0.4 µg of each of the plasmids pcDNA6.2-gw-EmGFP-miRNA-GRIK2.4,pcDNA6.2-gw-EmGFP-miRNA-GRIK2.5, pcDNA6.2-gw-EmGFP-miRNA-GRIK2.6, pcDNA6.2-gw-EmGFP-miRNA-GRIK2.7, and the control plasmid

pcDNA6.2-gw-EmGFP-miRNA-lacZ. One well of cells was transfected with only the pd-mCherry-GRIK2 plasmid. The plasmids were added to 0.3M $CaCl_2$ (25µl/well) before 2xHBS (280mM NaCl, 10mM KCl, 1.5mM Na_2HPO_4, 12mM D-glucose, 50mM HEPES (acid free), pH 7.05) (25µl/well) was added, and it was mixed well. The solutions incubated for five-ten minutes before they were added to the wells drop by drop. The plate was stirred gently, and then incubated in 37°C for 6 hours before the medium was aspirated, the cells were rinsed with DPBS+ buffer, and new medium (1 ml/well) was added.

After two days, the cells were fixed with 4% paraformaldehyde in 0.1M phosphate buffer for 30 minutes, and then washed with DPBS. The cells were then ready to be analyzed with a fluorescent microscope. The transfection experiment was replicated.

2.3.4 Imaging the EmGFP and mCherry expression

The digital image acquisition software AxioVision 4.6 (Zeiss, Oberkochen, Germany)[7] was used to take fluorescence images of the mCherry and the EmGFP expression in each well with a fluorescent microscope (Axiovert 40 CFL, Zeiss, Oberkochen, Germany). The images were taken with a 10x objective with 1 second exposure with a constant condition for all the images.

2.3.5 Analyzing by ImageJ

To quantify fluorescence intensity of mCherry and EmGFP the pixel value in each image was analyzed by the ImageJ software (NIH)[8]. To deal with variations in the background pixel value among images, and within each image, the average pixel values of the whole image and four background areas in each picture (two in a corner and two in the middle, in which no mCherry-positive cells existed) were measured for the mCherry expression. The average background pixel value was subtracted from the total image pixel value in each picture, and the subtracted value was normalized by dividing it by the average background value. For each of the shRNA plasmids and the controls, measurements from seven different images in the first experiment and five different images in the second experiment were used. For the EmGFP expression it was not possible to measure the background pixel value because the images were completely filled with GFP-expressing cells resulting in no background area.

[7] http://www.zeiss.de/C12567BE0045ACF1/Contents-Frame/668C9FDCBB18C6E2412568C10045A72E
[8] http://rsbweb.nih.gov/ij/

Measurements from two different images from each of the miRNA-GRIK2 plasmids and four different images from the miRNA-lacZ control were used in the first experiment, and five different images from each of the miRNA-GRIK2/lacZ plasmids were used in the second experiment. To quantify variations in cell morphology in the EmGFP fluorescence, round cells were counted in each image. The roundness criteria of cells were a subjective judgment, but since I did all the counting at the same time the same evaluation applied to all. The total cell number was measured by using the "find maxima" function of ImageJ to find all maximum points with a noise tolerance of 10. The percentage of round cells in total cell number was calculated. The statistical analyzes (ANOVA and post-hoc LSD test) were performed by the software PASW Statistics 18. The percentage reduction of the mCherry expression caused by the miRNA-GRIK2 plasmids was calculated by using the average of all measurements from the control mCherry-GRIK2 + miRNA-lacZ as a baseline (100%).

3. Results

3.1 Down-regulation by the miRNA-GRIK2 plasmids *in vitro*

The down-regulation effect of the four different miRNA-GRIK2 shRNA plasmids on expression of mCherry-GRIK2 fusion protein was examined by measuring the mCherry fluorescence in cells co-transfected with pd-mCherry-GRIK2 and each of the miRNA-GRIK2 or -lacZ plasmids (Figure 9). Clear reduction in mCherry fluorescence intensity was observed in cells transfected with the plasmids miRNA-GRIK2.5 and miRNA-GRIK2.6 in comparison with cells transfected with the control miRNA-lacZ in both the first and the second experiment, indicating that these two shRNAs had a successfully RNAi of the GRIK2 gene.

To quantify the RNAi effect of shRNAs, we measured the intensity of mCherry fluorescence in each sample using ImageJ. One-way ANOVA showed that the normalized pixel value was significantly different among groups both in the first experiment ($F_{(5, 36)}$= 34.42, p< 0.01) and in the replication ($F_{(5,24)}$= 20.62, p<0.01). The LSD post-hoc comparisons of the groups in the first experiment indicate that the pixel value was significantly lower in cells transfected with three of the plasmids (Figure 10); pcDNA6.2-gw-EmGFP-miRNA-GRIK2.5 (mean (M)=0.26, 95% confidence interval (CI) for the mean [0.21, 0.31], p<0.01), pcDNA6.2-gw-EmGFP-miRNA-GRIK2.6 (M=0.08, 95% CI [0.01, 0.15], p<0.01), and pcDNA6.2-gw-EmGFP-miRNA-GRIK2.7 (M=0.92, 95% CI [0.73, 1.11], p<0.01) compared to the control pcDNA6.2-gw-EmGFP-miRNA-lacZ (M=1.5, 95% CI [1.05, 1.95]). The normalized pixel value was not significantly lower in cells transfected with the plasmid pcDNA6.2-gw-EmGFP-miRNA-GRIK2.4 (M=1.48, 95% CI [1.16, 1.80], p=0.91). Compared with mCherry-GRIK2 + miRNA-lacZ, mCherry-GRIK2 + miRNA-GRIK2.5 showed a reduction of 82.7%, mCherry-GRIK2 + miRNA-GRIK2.6 showed a reduction of 94.4%, and mCherry-GRIK2 + miRNA-GRIK2.7 showed a reduction of 38.3%. The mCherry fluorescence was not significantly different between the two controls, cells co-transfected with mCherry-GRIK2 and miRNA-lacZ and cells with the mCherry-GRIK2 alone (M=1.39, 95% CI [1.12, 1.65], p=0.47).

In the replication of the experiment the LSD post-hoc comparisons of the groups indicate that all of the miRNA-GRIK2 plasmids gave a significant down-regulation of the mCherry fluorescence (Figure 11); pcDNA6.2-gw-EmGFP-miRNA-GRIK2.4 (M=2.29, 95% CI [1.40, 3.19], p<0.01), pcDNA6.2-gw-EmGFP-miRNA-GRIK2.5 (M=0.32, 95% CI [0.20, 0.44], p<0.01), pcDNA6.2-gw-EmGFP-miRNA-GRIK2.6 (M=0.09, 95% CI [-0.01, 0.18], p<0.01),

and pcDNA6.2-gw-EmGFP-miRNA-GRIK2.7 (M=1.75, 95% CI [1.34, 2.16], p<0.01) compared to the control pcDNA6.2-gw-EmGFP-miRNA-lacZ (M=4.94, 95% CI [3.87, 6.00]). With mCherry-GRIK2 + miRNA-lacZ as a 100% baseline, mCherry-GRIK2 + miRNA-GRIK2.4 showed a reduction of 53.5%, mCherry-GRIK2 + miRNA-GRIK2.5 showed a reduction of 93.6%, mCherry-GRIK2 + miRNA-GRIK2.6 showed a reduction of 98.2%, and mCherry-GRIK2 + miRNA-GRIK2.7 showed a reduction of 64.5%. The mCherry fluorescence was not significantly different between the two controls, cells co-transfected with mCherry-GRIK2 and miRNA-lacZ and cells with the mCherry-GRIK2 alone (M=4.26, 95% CI [2.68, 5.84], p=0.14).

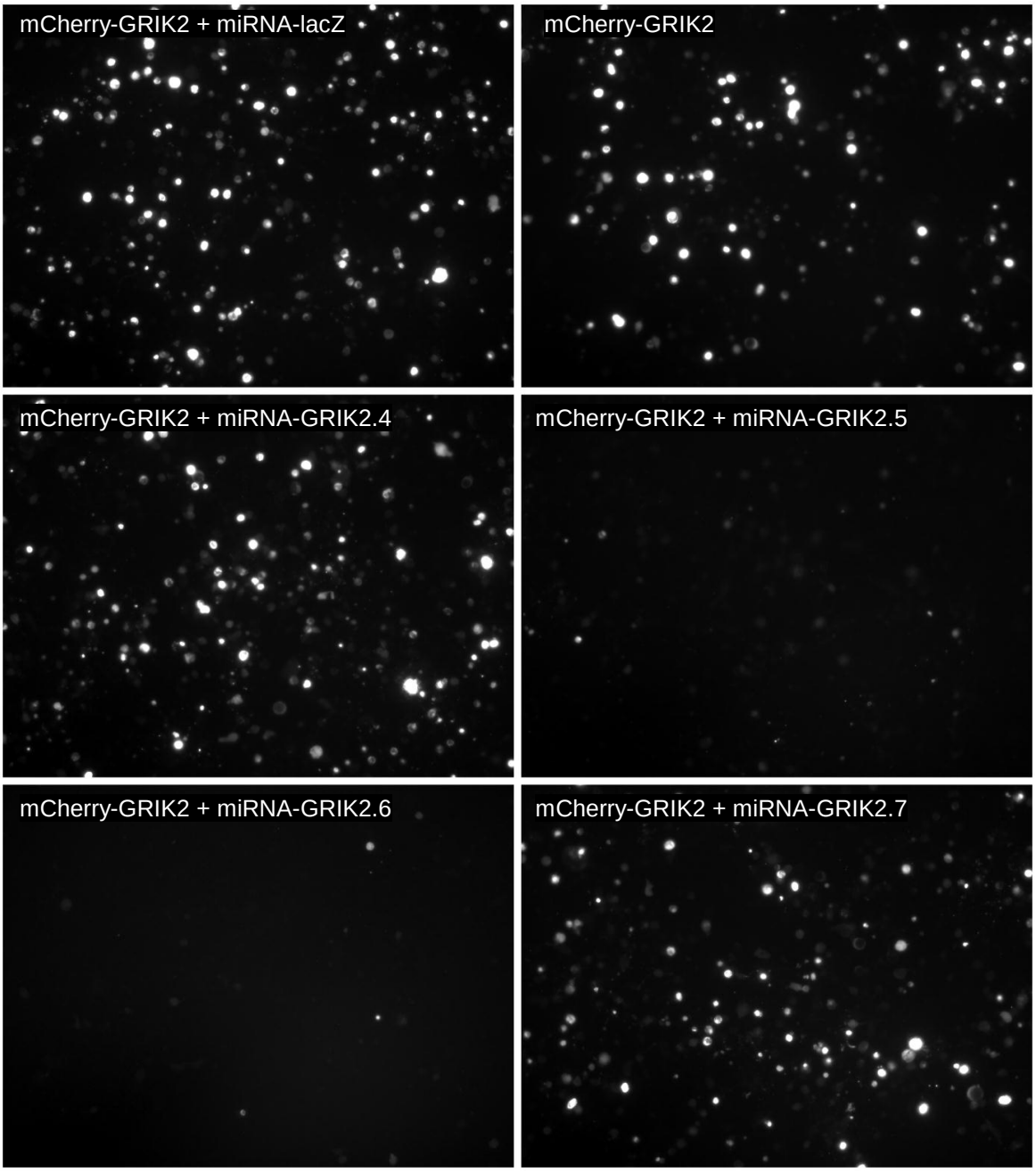

Figure 9. Representative images of the mCherry fluorescence in cells transfected with pd-mCherry-GRIK2 and in cells co-transfected with pd-mCherry-GRIK2 and each of the pcDNA6.2-gw-EmGFP-miRNA-lacZ/GRIK2 plasmids.

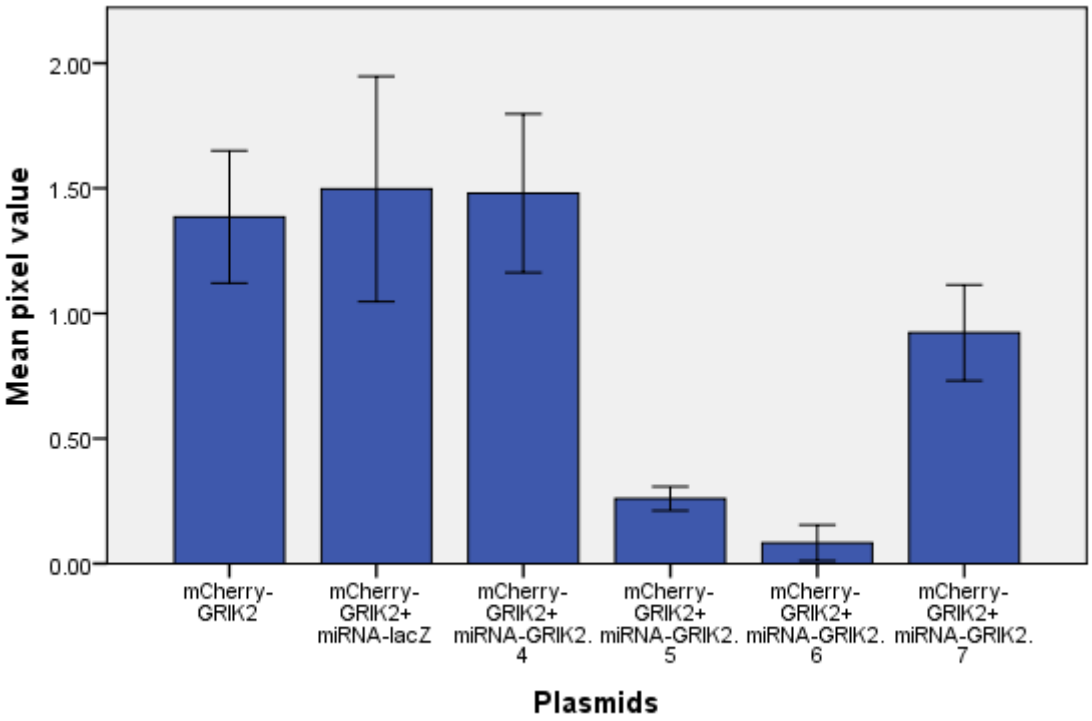

Figure 10. The graph from the first experiment show the mean pixel value of mCherry fluorescence intensity in cells transfected with the pd-mCherry-GRIK2 plasmid alone and in each of the cells co-transfected with pd-mCherry-GRIK2 and one of the pcDNA6.2-gw-EmGFP-miRNA-lacZ/GRIK2 plasmids. Error bars of 95% confidence interval.

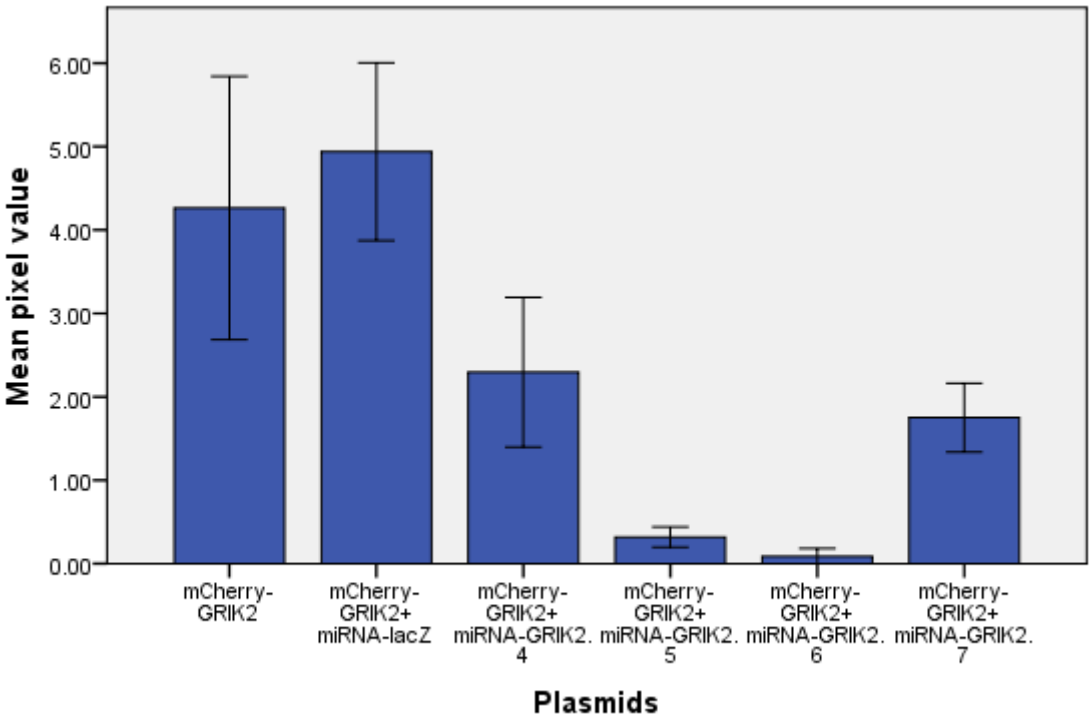

Figure 11. The graph from the second experiment show the mean pixel value of mCherry fluorescence intensity in cells transfected with the pd-mCherry-GRIK2 plasmid alone and in each of the cells co-transfected with pd-mCherry-GRIK2 and one of the pcDNA6.2-gw-EmGFP-miRNA-lacZ/GRIK2 plasmids. Error bars of 95% confidence interval.

3.2 The EmGFP expression level

The miRNA-GRIK2 plasmids permit visual identification of cells expressing the shRNAs through co-cistonic expression of EmGFP. To find out if the transfections of the miRNA-GRIK2 plasmids were successful, the expression level of EmGFP was examined using fluorescence intensity in all of the co-transfected cells (Figure 12). The mean EmGFP fluorescence intensity in all of the co-transfected cells in the first experiment (Figure 13) and the second experiment (Figure 14) were quantified. One-way ANOVA showed that the mean EmGFP fluorescence intensity was significantly different among all groups in both the first experiment ($F_{(4, 7)}$= 47.83, p< 0.01) and in the second experiment ($F_{(4, 20)}$= 63.44, p< 0.01). The LSD post-hoc comparisons of the groups in the first experiment indicate that the control pcDNA6.2-gw-EmGFP-miRNA-lacZ (M=44.30, 95% CI [28.32, 60.29]) had a significantly lower EmGFP expression compared to all of the miRNA-GRIK2 plasmids; pcDNA6.2-gw-EmGFP-miRNA-GRIK2.4 (M=102.66, 95% CI [35.47, 169.85], p<0.01), pcDNA6.2-gw-EmGFP-miRNA-GRIK2.5 (M=128.44, 95% CI [67.67, 189.21], p<0.01), pcDNA6.2-gw-EmGFP-miRNA-GRIK2.6 (M=129.90, 95% CI [71.17, 188.62], p<0.01), and pcDNA6.2-gw-EmGFP-miRNA-GRIK2.7 (M=91.62, 95% CI [4.05, 179.19], p<0.01). In the second experiment the LSD post-hoc comparisons of the groups indicate that the control pcDNA6.2-gw-EmGFP-miRNA-lacZ (M=32.20, 95% CI [26.49, 37.91]) had a significantly lower EmGFP expression compared to three of the miRNA-GRIK2 plasmids; pcDNA6.2-gw-EmGFP-miRNA-GRIK2.4 (M=66.79, 95% CI [48.95, 84.64], p<0.01), pcDNA6.2-gw-EmGFP-miRNA-GRIK2.5 (M=61.78, 95% CI [57.92, 65.64], p<0.01), and pcDNA6.2-gw-EmGFP-miRNA-GRIK2.6 (M=148.50, 95% CI [119.64, 177.35], p<0.01), but not pcDNA6.2-gw-EmGFP-miRNA-GRIK2.7 (M=39.99, 95% CI [29.84, 50.14], p=0.35).

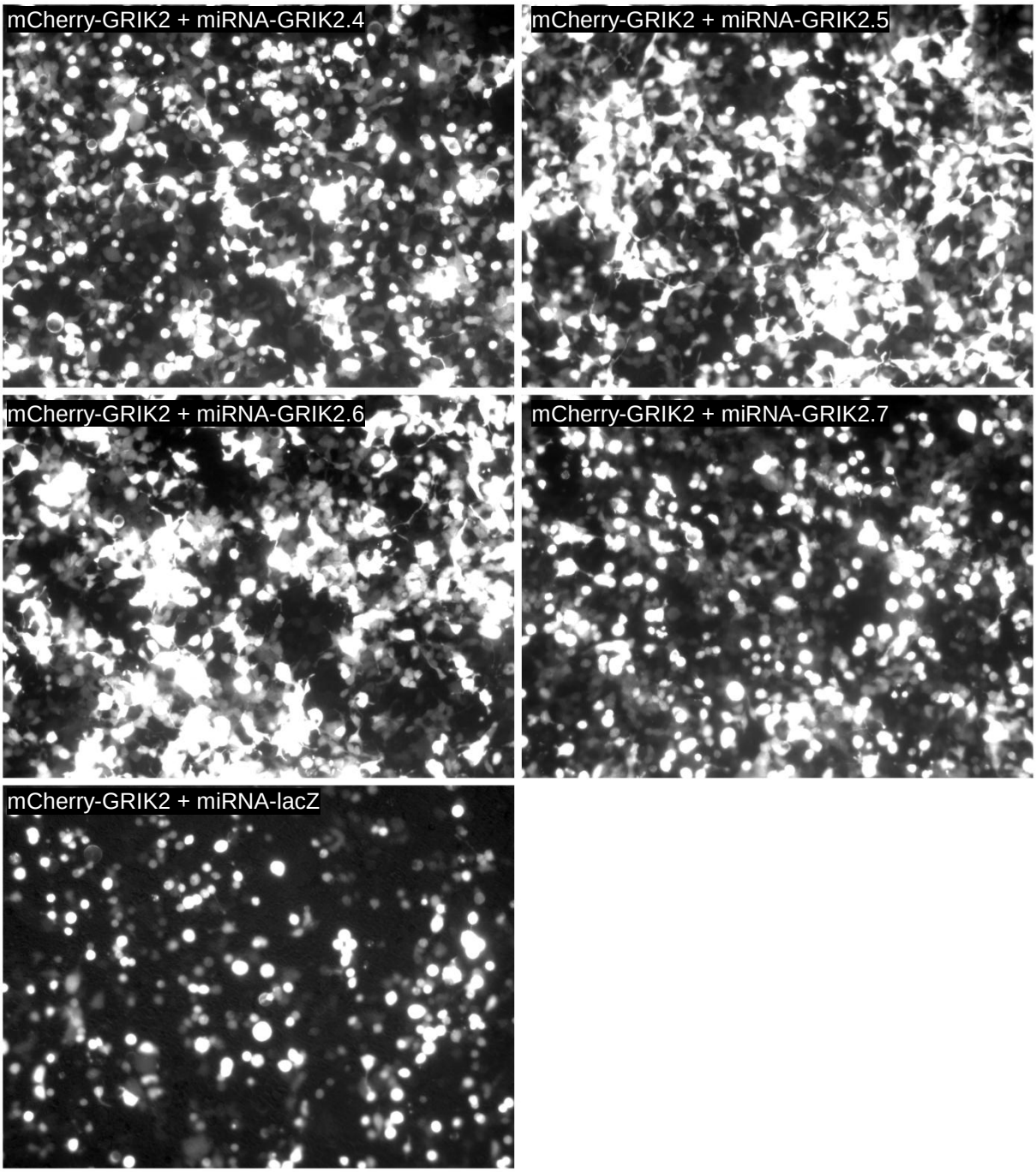

Figure 12. Representative images of the EmGFP fluorescence in each of the cells co-transfected with pd-mCherry-GRIK2 and pcDNA6.2-gw-EmGFP-miRNA-GRIK2/lacZ.

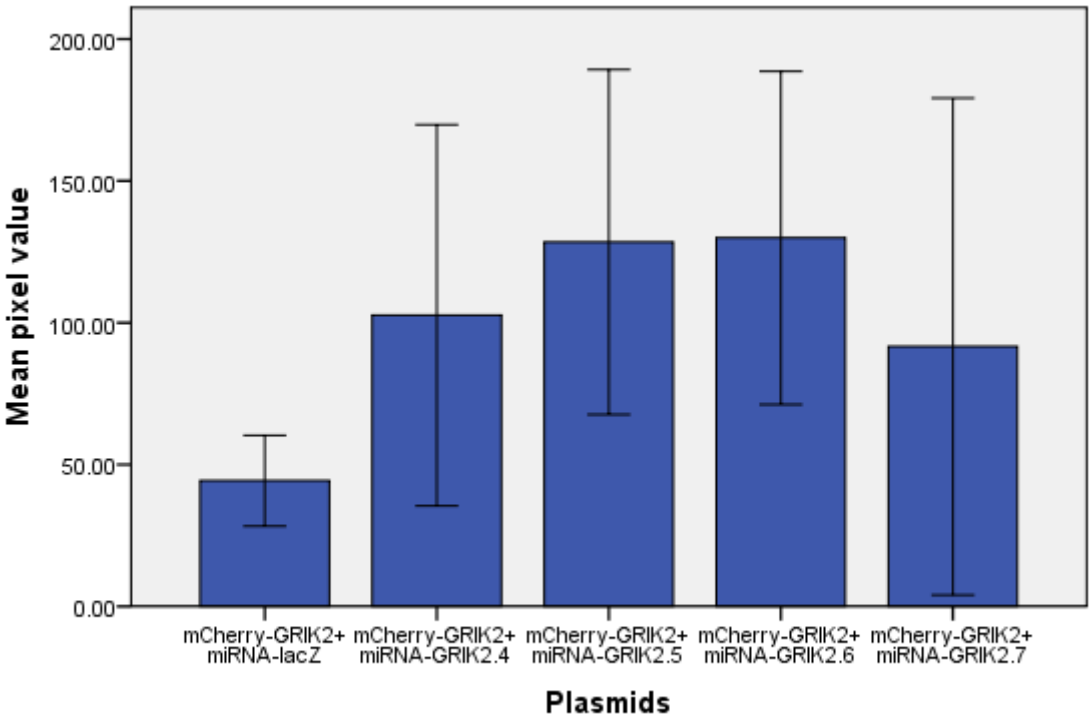

Figure 13. A graph of the mean EmGFP fluorescence intensity in all of the cells co-transfected with pd-mCherry-GRIK2 and pcDNA6.2-gw-EmGFP-miRNA-GRIK2/lacZ from the first experiment. Error bars of 95% confidence interval.

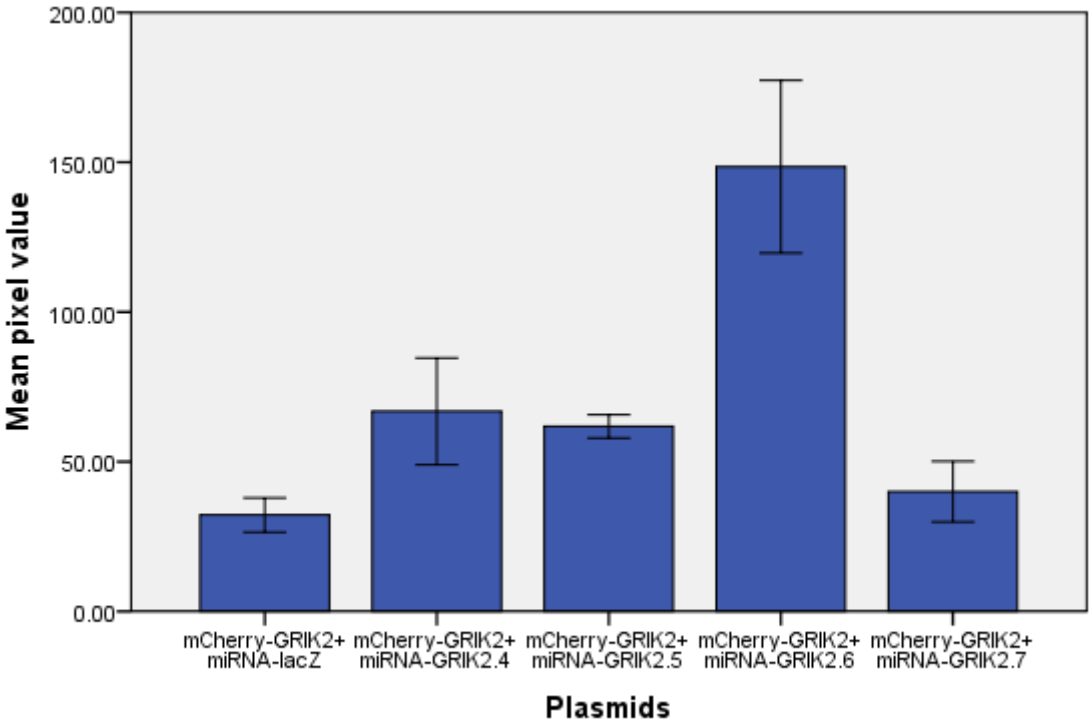

Figure 14. A graph of the mean EmGFP fluorescence intensity in all of the cells co-transfected with pd-mCherry-GRIK2 and pcDNA6.2-gw-EmGFP-miRNA-GRIK2/lacZ from the second experiment. Error bars of 95% confidence interval.

3.3 Cell morphology visualized in the EmGFP fluorescence

Another observation was a difference in cell morphology visualized by the EmGFP fluorescence. Cells transfected with miRNA-lacZ had a rounder shape (Figure 15A) compared to the cells with miRNA-GRIK2.6 (Figure 15B) and miRNA-GRIK2.5. The miRNA-GRIK2.4 and miRNA-GRIK2.7 also had a similar round shape of some of the cells, though in a lesser extent. This pattern was observed in both replications of the experiments. Percentage of round cells was calculated and compared among the groups in the first experiment (Figure 16) and in the second experiment (Figure 17). One-way ANOVA showed that the percentage of round cells was significantly different among all the co-transfected groups in both the first experiment ($F_{(4,7)}=7.58$, $p<0.05$) and in the second experiment ($F_{(4,18)}=63.11$, $p<0.01$). In the first experiments the LSD post-hoc comparisons showed that pcDNA6.2-gw-EmGFP-miRNA-lacZ has significantly higher percentage of round cells (M=7.90, 95% CI [3.34, 12.47]) than three of the other plasmids; pcDNA6.2-gw-EmGFP-miRNA-GRIK2.5 (M=0.60, 95% CI [0.18, 1.02], $p<0.01$), pcDNA6.2-gw-EmGFP-miRNA-GRIK2.6 (M=0.10, 95% CI [-0.47, 1.39], $p<0.01$), and pcDNA6.2-gw-EmGFP-miRNA-GRIK2.7 (M=3.64, 95% CI [1.75, 5.52], $p<0.05$), but not pcDNA6.2-gw-EmGFP-miRNA-GRIK2.4 (M=4.90, 95% CI [-2.81, 12.60], $p=0.11$). None of the other groups differed significantly from the other groups. In the second experiment the LSD post-hoc comparisons showed that pcDNA6.2-gw-EmGFP-miRNA-lacZ has significantly higher percentage of round cells (M=14.51, 95% CI [11.86, 17.16]) than all of the other plasmids; pcDNA6.2-gw-EmGFP-miRNA-GRIK2.4 (M=4.55, 95% CI [3.75, 5.34], $p<0.01$), pcDNA6.2-gw-EmGFP-miRNA-GRIK2.5 (M=1.08, 95% CI [0.55, 1.61], $p<0.01$), pcDNA6.2-gw-EmGFP-miRNA-GRIK2.6 (M=0.57, 95% CI [0.30, 0.83], $p<0.01$), and pcDNA6.2-gw-EmGFP-miRNA-GRIK2.7 (M=7.03, 95% CI [4.17, 9.89], $p<0.01$). The miRNA-GRIK2.5 and miRNA-GRIK2.6 plasmids were the only plasmids that did not significantly differ from each other in the percentage amount of round cells.

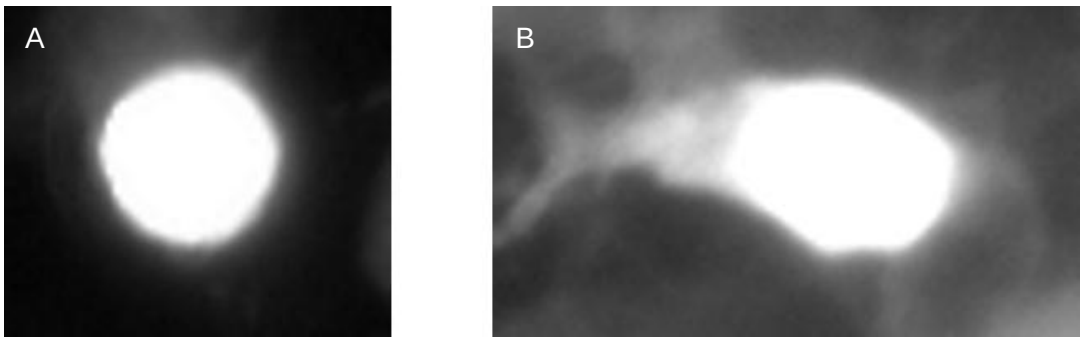

Figure 15. Cell morphology visualized in the EmGFP fluorescence. A) A round cell from the control mCherry-GRIK2 + miRNA-lacZ co-transfection. B) A non-round cell from the mCherry-GRIK2 + miRNA-GRIK2.6 co-transfection.

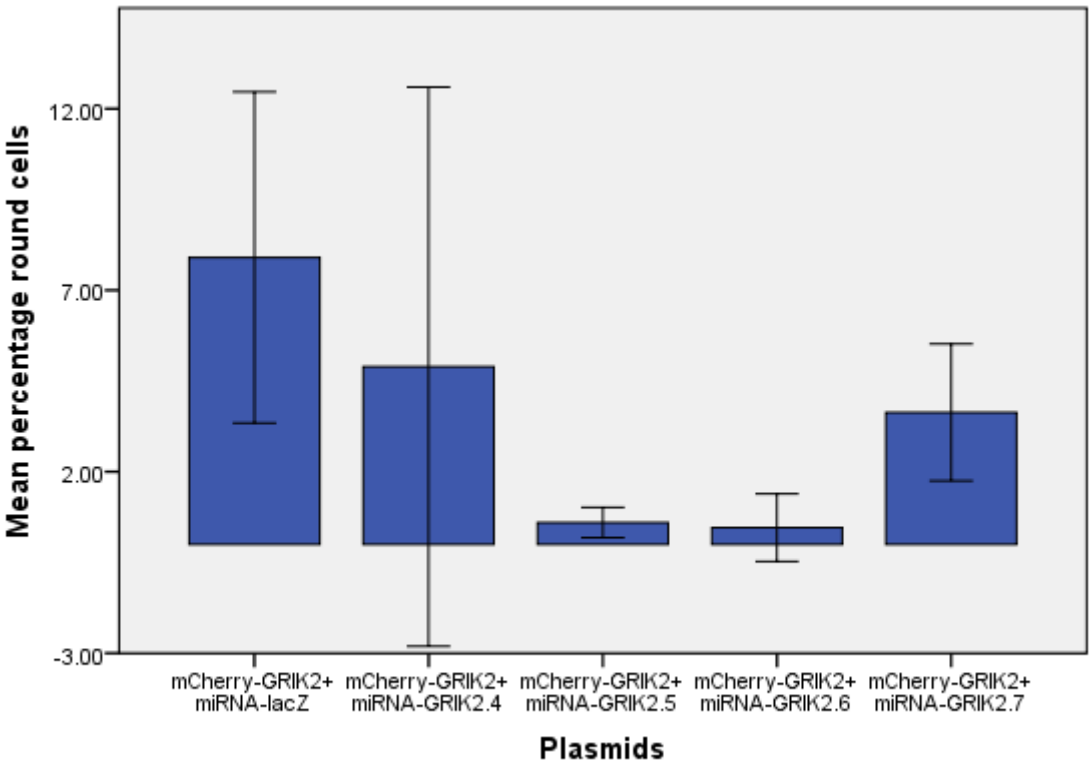

Figure 16. Graph showing the mean number of percentage round cells in the total cell number visualized in the EmGFP fluoresence in the co-transfected cells in the first experiment. Error bars of 95% confidence interval.

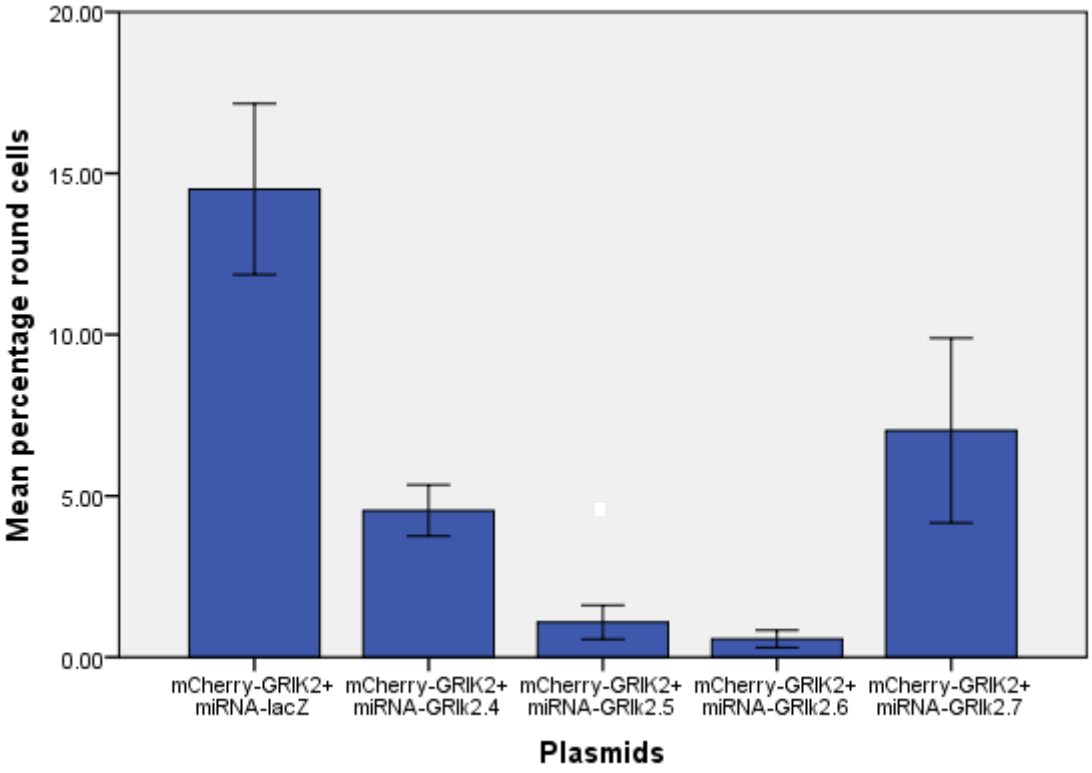

Figure 17. Graph showing the mean number of percentage round cells in the total cell number visualized in the EmGFP fluoresence in the co-transfected cells in the second experiment. Error bars of 95% confidence interval.

4. Discussion

In this thesis I have established a fluorescence-based cell culture assay to easily determine RNAi effects of shRNAs, and by using this assay, I have identified two shRNA sequences that achieved 90% down-regulation of the GRIK2 gene expression *in vitro* in two replications of the experiment.

4.1 Versatility of the fluorescence-based cell culture assay

The fluorescence-based cell culture assay established in this thesis can be used to test shRNA sequences for silencing of any other genes of interest. In this screening assay, the shRNA plasmids were co-transfected with a plasmid containing a gene of interest fused to the fluorescent protein mCherry, which made it possible to determine the down-regulation of the gene of interest by measuring the mCherry fluorescence intensity from transfected cells, without using any additional biochemical or molecular biology methods, such as Western blot or quantitative PCR. The shRNA plasmids contain another fluorescent reporter gene, EmGFP, which could be used to confirm the successful transfection of the shRNA plasmids. A plasmid with shRNA against the lacZ gene was used as a control. Since eukaryotic cell lines do not contain this gene, the miRNA-lacZ gene will be transcribed and processed similar to the other shRNA plasmids, but the shRNA with lacZ will not perform RNAi and the mCherry fluorescence in the co-transfection with the mCherry fusion gene plasmid should not be affected. That is consistent with this experiment since there was no significantly difference in the mCherry fluorescence intensity between the cells co-transfected with mCherry-GRIK2 + miRNA-lacZ and the cells transfected with mCherry-GRIK2 alone. The mCherry fluorescence intensity in the co-transfection with miRNA-lacZ was therefore used as a baseline, and the mCherry fluorescence intensities in the co-transfections with the different miRNA-GRIK2 plasmids were compared to this. An advantage of this procedure is its versatility to any gene of interest. To make the mCherry fusion protein, we have made a mCherry fusion gene plasmid compatible to the Invitrogen's Gateway system-compatible destination vector. The Gateway Technology is a universal cloning method that takes advantage of the site-specific recombination properties of bacteriophage lambda (Landy, 1989) to provide a rapid and efficient way to move the DNA sequence of interest into multiple vector systems. Using a library of many genes of interest in Gateway donor vectors, which is available from some companies like imaGenes (Berlin, Germany) or GeneCopoeia (Rockville/MD, USA), it is easy to construct a library of plasmids encoding mCherry fusion

proteins with different genes. shRNA plasmids are also easy to make by using a kit from Invitrogen, as the one used in this thesis.

4.2 Successful down-regulation by two shRNA sequences

The results from the first analyses of the shRNA assay showed that the reduction of the mCherry fluorescence compared to the baseline was 82.7% by miRNA-GRIK2.5, 94.4% by miRNA-GRIK2.6, and 38.3% by miRNA-GRIK2.7. The miRNA-GRIK2.4 did not have a statistically significant down-regulation effect. In the replication of the experiment all of the shRNA plasmids resulted in a significantly down-regulation of the mCherry-GRIK2 fusion protein. The miRNA-GRIK2.4 gave a reduction of 53.5%, miRNA-GRIK2.5 gave a reduction of 93.5%, miRNA-GRIK2.6 gave a reduction of 98.2%, and miRNA-GRIK2.7 gave a reduction of 64.5%. The variations in the results can arise from different conditions in the experiments. Several replications could have been performed to get a more reliable result, but the aim of this experiment was to identify one or two shRNAs that can be used in further *in vivo* experiments. Both experiments showed stable down-regulations of average 90% by the plasmids miRNA-GRIK2.5 and miRNA-GRIK2.6, which are the shRNA plasmids that will be used for further experiments. The other two plasmids, miRNA-GRIK2.7 and miRNA-GRIK2.4, were less effective and had a more variable down-regulation.

4.3 Differences in EmGFP expression level and cell morphology

An observation from the experiment is that the various miRNA plasmids showed a different expression level of EmGFP fluorescence. The miRNA-lacZ plasmid had lower expression of EmGFP compared to all of the miRNA-GRIK2 plasmids in the first experiment and to all of the miRNA-GRIK2 plasmids except the miRNA-GRIK2.7 plasmid in the second experiment. The confidence interval of the mean EmGFP fluorescence is very large in the first experiment because it is only two measurements from each of the cells co-transfected with the miRNA-GRIK2 plasmids, but the miRNA-lacZ plasmid still shows a significantly lower EmGFP expression level than the other plasmids. This may be due to different amount of plasmids inside cells caused by difference in transfection efficiency or some other reasons. Because two replicated experiments showed similar variations (lower in controls), the difference would not be caused by random variation of transfection efficiency. Another possibility is that the measured concentration of maxiprep samples of the plasmid was not accurate. This possibility cannot be excluded, and estimated efficiency of RNAi (%reduction in mCherry fluorescence) may not be accurate. However, the amount of transfected mCherry-GRIK2 plasmid should be equal among all groups, because a common maxiprep sample of

mCherry-GRIK2 plasmid was used for all groups. This means that difference in mCherry fluorescence between groups was caused by different efficiency of RNAi associated with different shRNA sequences. Although the estimated reduction may not be accurate, the conclusion that GRIK2.5 and GRIK2.6 shRNA sequences are the most effective is still valid.

Another observation visualized in the EmGFP fluorescence is a positive correlation between the mCherry level and percentage of round cells, which suggests that either the expression of mCherry or GRIK2 makes the cells round. We have expressed mCherry alone in cells in other experiments in the lab and have not observed round cells, so it is more likely due to GRIK2 expression. In the quantified data the EmGFP expression level has a negative correlation with the mCherry level and the percentage of round cells. That is also my impression in individual cell level observed in the microscope. This implies that the GRIK2 expression makes cells round and reduces the EmGFP expression. If the GRIK2 expression can change something like cell shape, it is no surprise that it changes the (CMV) promoter activity or protein degradation. Such side effects of gene expression could make this assay difficult to use for some genes. In this experiment however, it was not a problem because the GRIK2 expression reduced the EmGFP expression. But if a gene increase the level of EmGFP expression, then it would not be possible to tell whether the difference in mCherry level is due to the specific down-regulation of the shRNAs or differences in transfection efficiency.

4.4 Evaluation of the analytical method

The measurements of the mCherry and EmGFP fluorescence intensities were performed by analyzing the pixel value in each image by the ImageJ software. The background brightness varied among the images, and within each image the background was always darker in the corners compared to the centre of the image because of uneven illumination of excitation lights over the field. To deal with this issue I measured the background pixel value in the mCherry fluorescence on four different positions in each image, two in the corners and two in the centre of the image, and subtracted the average value from the value of the whole image. The pixel value was then normalized by dividing by the average background pixel value. I tried to measure the background in the same positions in every image, but it could not be done since I had to avoid cells that expressed the fluorescence. The exact background intensity from the brightest area could therefore not be measured if many cells were located in that area. Since seven images were analyzed from each group in the first experiment and five in the second experiment, this variance should be evenly distributed. It was not possible

to measure the background brightness in the EmGFP fluorescence because the images were completely filled with GFP-expressing cells resulting in no background area. The results from the EmGFP fluorescence analyses are therefore not subtracted by background pixel values, but the quantification seems to well reflect the observations seen in the microscope. Another way we tried was by comparing the mCherry fluorescence with the EmGFP fluorescence in each cell in the same positions in each image. The percentage of EmGFP fluorescent cells that also show mCherry fluorescence can be measured. An issue with this method is the high expression of EmGFP, which made it impossible to separate the cells from the others. A possibility could have been to incubate the cells a shorter time or add fewer cells to the wells and do the analyses before the cells were confluent. Then it could have been possible to analyze the cells separately. Another way to do the analyses could have been to use the EmGFP fluorescence intensity in the whole image as a baseline, and normalize the mCherry fluorescence intensity by the baseline value. A problem with that method is that the EmGFP fluorescence intensity is different among the groups in this experiment, which would make the percentage of reduction even higher as a result of other factors than the down-regulation by the shRNAs.

4.5 Further work

The ultimate goal of this project is to establish a role of the kainate receptor in development of mossy fibres in adult born dentate granule cells. The two miRNA-GRIK2 sequences with the best down-regulation effect will be used to inhibit the expression of GRIK2 in young adult born neurons *in vivo*. This can be performed by using a retrovirus vector, which specifically affects dividing cells, and inject it into the dentate gyrus of adult mice. Since we have used mice miRNA-GRIK2 sequences, we have to use mice for further experiments. By using different survival periods after injection of the viral vector, adult born neurons of different ages can be studied and a specific timeline for the development of the newborn neurons can be established. Morphological characteristics, like filopodia, can be studied at different time points. The morphology can be compared in mice with and without the kainate receptor silencing. Another experiment, which is being initiated in the lab, is to test the kainate receptor subunits GRIK3 and GRIK5 in the same way, and find out if post-transcriptional silencing of the other subunits would result in different findings. The screening assay established in this thesis will be used in that experiment. A plasmid with miRNA sequences for several of the kainate receptor subunits can be incorporated into the same vector plasmid, and we may be able to achieve a successful knock-down of the kainate receptor in newborn neurons. By using this approach, another experiment could be performed to test mice in behavioural tasks to find out if the absence of kainate receptors affects their ability of

learning or memory. In this experiment a retrovirus vector would not be suitable because it only infects a minor population of new neurons, but several other methods are possible to use. One method we could use is to transfer the shRNA plasmids with adeno-associated virus (AAV) vectors. To get the specific expression of shRNAs in young granule cells we can use POMC-Cre mice, which use the pro-opiomelanocortin (POMC) promoter to express Cre recombinase specifically in newborn neurons. The Cre/loxP system can be used for site-specific recombination of double floxed shRNA genes (the shRNA gene can be flanked with the loxP sites), and new neurons that express Cre recombinase from the cell specific promotor POMC get a specific expression of the shRNAs (Bucholtz, 2008).

4.6 Conclusion

In conclusion, we have established a fluorescence-based cell culture assay to easily determine RNA interference effects of shRNAs, which can be easily adaptable for any gene of interest. And by using this assay, I have identified two shRNA sequences that successfully down-regulated the kainate receptor subunit GRIK2 expression by an average of 90%. The sequences will be used in further studies that aim to identify the role of the kainate receptor in development of newborn dentate granule cells.

5. References

Acsady, L., Kamondi, A., Sik, A., Freund, T., & Buzsaki, G. (1998). GABAergic cells are the major postsynaptic targets of mossy fibers in the rat hippocampus. *Journal of Neuroscience, 18*(9), 3386-3403.

Altman, J. (1969a). Autoradiographic and histological studies of postnatal neurogenesis. 3. Dating the time of production and onset of differentiation of cerebellar microneurons in rats. *Journal of Comparative Neurology, 136*(3), 269-293.

Altman, J. (1969b). Autoradiographic and histological studies of postnatal neurogenesis. IV. Cell proliferation and migration in the anterior forebrain, with special reference to persisting neurogenesis in the olfactory bulb. *Journal of Comparative Neurology, 137*(4), 433-457.

Altman, J., & Das, G. D. (1965a). Autoradiographic and histological evidence of postnatal hippocampal neurogenesis in rats. *Journal of Comparative Neurology, 124*(3), 319-335.

Altman, J., & Das, G. D. (1965b). Post-natal origin of microneurones in the rat brain. *Nature, 207*(5000), 953-956.

Alvarez, V. A., Ridenour, D. A., & Sabatini, B. L. (2006). Retraction of synapses and dendritic spines induced by off-target effects of RNA interference. *Journal of Neuroscience, 26*(30), 7820-7825.

Amaral, D. G., Scharfman, H. E., & Lavenex, P. (2007). The dentate gyrus: fundamental neuroanatomical organization (dentate gyrus for dummies). *Progress in Brain Research, 163*, 3-22.

Amaral, D. G., & Witter, M. P. (1989). The three-dimensional organization of the hippocampal formation: a review of anatomical data. *Neuroscience, 31*(3), 571-591.

Ambros, V. (2001). microRNAs: tiny regulators with great potential. *Cell, 107*(7), 823-826.

Bernstein, E., Caudy, A. A., Hammond, S. M., & Hannon, G. J. (2001). Role for a bidentate ribonuclease in the initiation step of RNA interference. *Nature, 409*(6818), 363-366.

Bliss, T. V., & Lomo, T. (1973). Long-lasting potentiation of synaptic transmission in the dentate area of the anaesthetized rabbit following stimulation of the perforant path. *J Physiol, 232*(2), 331-356.

Bucholtz, F. (2008). Principles of site-specific recombinase (SSR) technology. *J Vis Exp*(15).

Bull, N. D., & Bartlett, P. F. (2005). The adult mouse hippocampal progenitor is neurogenic but not a stem cell. *Journal of Neuroscience, 25*(47), 10815-10821.

Cameron, H. A., & McKay, R. D. (2001). Adult neurogenesis produces a large pool of new granule cells in the dentate gyrus. *Journal of Comparative Neurology, 435*(4), 406-417.

Cameron, H. A., Woolley, C. S., McEwen, B. S., & Gould, E. (1993). Differentiation of newly born neurons and glia in the dentate gyrus of the adult rat. *Neuroscience, 56*(2), 337-344.

Castillo, P. E., Malenka, R. C., & Nicoll, R. A. (1997). Kainate receptors mediate a slow postsynaptic current in hippocampal CA3 neurons. *Nature, 388*(6638), 182-186.

Chittajallu, R., Braithwaite, S. P., Clarke, V. R., & Henley, J. M. (1999). Kainate receptors: subunits, synaptic localization and function. *Trends in Pharmacological Sciences, 20*(1), 26-35.

Chung, K. H., Hart, C. C., Al-Bassam, S., Avery, A., Taylor, J., Patel, P. D., et al. (2006). Polycistronic RNA polymerase II expression vectors for RNA interference based on BIC/miR-155. *Nucleic Acids Res, 34*(7), e53.

Cogoni, C., & Macino, G. (1997). Isolation of quelling-defective (qde) mutants impaired in posttranscriptional transgene-induced gene silencing in Neurospora crassa. *Proceedings of the National Academy of Sciences of the United States of America, 94*(19), 10233-10238.

Cogoni, C., Romano, N., & Macino, G. (1994). Suppression of gene expression by homologous transgenes. *Antonie Van Leeuwenhoek, 65*(3), 205-209.

Contractor, A., Swanson, G. T., Sailer, A., O'Gorman, S., & Heinemann, S. F. (2000). Identification of the kainate receptor subunits underlying modulation of excitatory synaptic transmission in the CA3 region of the hippocampus. *Journal of Neuroscience, 20*(22), 8269-8278.

Cullen, B. R. (2005). RNAi the natural way. *Nature Genetics, 37*(11), 1163-1165.

Deng, W., Aimone, J. B., & Gage, F. H. (2010). New neurons and new memories: how does adult hippocampal neurogenesis affect learning and memory? *Nat Rev Neurosci, 11*(5), 339-350.

Deng, W., Saxe, M. D., Gallina, I. S., & Gage, F. H. (2009). Adult-born hippocampal dentate granule cells undergoing maturation modulate learning and memory in the brain. *Journal of Neuroscience, 29*(43), 13532-13542.

Du, T., & Zamore, P. D. (2005). microPrimer: the biogenesis and function of microRNA. *Development, 132*(21), 4645-4652.

Egebjerg, J., Bettler, B., Hermans-Borgmeyer, I., & Heinemann, S. (1991). Cloning of a cDNA for a glutamate receptor subunit activated by kainate but not AMPA. *Nature, 351*(6329), 745-748.

Eriksson, P. S., Perfilieva, E., Bjork-Eriksson, T., Alborn, A. M., Nordborg, C., Peterson, D. A., et al. (1998). Neurogenesis in the adult human hippocampus. *Nature Medicine, 4*(11), 1313-1317.

Fire, A., Xu, S., Montgomery, M. K., Kostas, S. A., Driver, S. E., & Mello, C. C. (1998). Potent and specific genetic interference by double-stranded RNA in Caenorhabditis elegans. *Nature, 391*(6669), 806-811.

Forster, E., Zhao, S., & Frotscher, M. (2006). Laminating the hippocampus. *Nat Rev Neurosci, 7*(4), 259-267.

Garcia, A. D., Doan, N. B., Imura, T., Bush, T. G., & Sofroniew, M. V. (2004). GFAP-expressing progenitors are the principal source of constitutive neurogenesis in adult mouse forebrain. *Nature Neuroscience, 7*(11), 1233-1241.

Ge, S., Goh, E. L., Sailor, K. A., Kitabatake, Y., Ming, G. L., & Song, H. (2006). GABA regulates synaptic integration of newly generated neurons in the adult brain. *Nature, 439*(7076), 589-593.

Gilbert, P. E., Kesner, R. P., & DeCoteau, W. E. (1998). Memory for spatial location: role of the hippocampus in mediating spatial pattern separation. *Journal of Neuroscience, 18*(2), 804-810.

Gilbert, P. E., Kesner, R. P., & Lee, I. (2001). Dissociating hippocampal subregions: double dissociation between dentate gyrus and CA1. *Hippocampus, 11*(6), 626-636.

Gould, E., Beylin, A., Tanapat, P., Reeves, A., & Shors, T. J. (1999). Learning enhances adult neurogenesis in the hippocampal formation. *Nature Neuroscience, 2*(3), 260-265.

Gould, E., Reeves, A. J., Fallah, M., Tanapat, P., Gross, C. G., & Fuchs, E. (1999). Hippocampal neurogenesis in adult Old World primates. *Proceedings of the National Academy of Sciences of the United States of America, 96*(9), 5263-5267.

Gould, E., Tanapat, P., Hastings, N. B., & Shors, T. J. (1999). Neurogenesis in adulthood: a possible role in learning. *Trends Cogn Sci, 3*(5), 186-192.

Hammond, S. M., Bernstein, E., Beach, D., & Hannon, G. J. (2000). An RNA-directed nuclease mediates post-transcriptional gene silencing in Drosophila cells. *Nature, 404*(6775), 293-296.

Herb, A., Burnashev, N., Werner, P., Sakmann, B., Wisden, W., & Seeburg, P. H. (1992). The KA-2 subunit of excitatory amino acid receptors shows widespread expression in brain and forms ion channels with distantly related subunits. *Neuron, 8*(4), 775-785.

Houser, C. R. (2007). Interneurons of the dentate gyrus: an overview of cell types, terminal fields and neurochemical identity. *Progress in Brain Research, 163*, 217-232.

Jessberger, S., Clark, R. E., Broadbent, N. J., Clemenson, G. D., Jr., Consiglio, A., Lie, D. C., et al. (2009). Dentate gyrus-specific knockdown of adult neurogenesis impairs spatial and object recognition memory in adult rats. *Learning and Memory, 16*(2), 147-154.

Jiao, Z., Zhang, Z. G., Hornyak, T. J., Hozeska, A., Zhang, R. L., Wang, Y., et al. (2006). Dopachrome tautomerase (Dct) regulates neural progenitor cell proliferation. *Developmental Biology, 296*(2), 396-408.
Jones, S. P., Rahimi, O., O'Boyle, M. P., Diaz, D. L., & Claiborne, B. J. (2003). Maturation of granule cell dendrites after mossy fiber arrival in hippocampal field CA3. *Hippocampus, 13*(3), 413-427.
Kaplan, M. S., & Hinds, J. W. (1977). Neurogenesis in the adult rat: electron microscopic analysis of light radioautographs. *Science, 197*(4308), 1092-1094.
Kempermann, G., Kuhn, H. G., & Gage, F. H. (1997). More hippocampal neurons in adult mice living in an enriched environment. *Nature, 386*(6624), 493-495.
Landy, A. (1989). Dynamic, structural, and regulatory aspects of lambda site-specific recombination. *Annual Review of Biochemistry, 58*, 913-949.
Lawrence, J. J., Grinspan, Z. M., & McBain, C. J. (2004). Quantal transmission at mossy fibre targets in the CA3 region of the rat hippocampus. *J Physiol, 554*(Pt 1), 175-193.
Lee, I., Yoganarasimha, D., Rao, G., & Knierim, J. J. (2004). Comparison of population coherence of place cells in hippocampal subfields CA1 and CA3. *Nature, 430*(6998), 456-459.
Lee, Y., Ahn, C., Han, J., Choi, H., Kim, J., Yim, J., et al. (2003). The nuclear RNase III Drosha initiates microRNA processing. *Nature, 425*(6956), 415-419.
Leutgeb, J. K., Leutgeb, S., Moser, M. B., & Moser, E. I. (2007). Pattern separation in the dentate gyrus and CA3 of the hippocampus. *Science, 315*(5814), 961-966.
Martin, S. J., & Morris, R. G. (2002). New life in an old idea: the synaptic plasticity and memory hypothesis revisited. *Hippocampus, 12*(5), 609-636.
McDermott, K. W., & Lantos, P. L. (1990). Cell proliferation in the subependymal layer of the postnatal marmoset, Callithrix jacchus. *Brain Research. Developmental Brain Research, 57*(2), 269-277.
Migliore, M. (2003). On the integration of subthreshold inputs from Perforant Path and Schaffer Collaterals in hippocampal CA1 pyramidal neurons. *Journal of Computational Neuroscience, 14*(2), 185-192.
Monaghan, D. T., & Cotman, C. W. (1982). The distribution of [3H]kainic acid binding sites in rat CNS as determined by autoradiography. *Brain Research, 252*(1), 91-100.
Monje, M. L., Mizumatsu, S., Fike, J. R., & Palmer, T. D. (2002). Irradiation induces neural precursor-cell dysfunction. *Nature Medicine, 8*(9), 955-962.
Morris, R. G., Schenk, F., Tweedie, F., & Jarrard, L. E. (1990). Ibotenate Lesions of Hippocampus and/or Subiculum: Dissociating Components of Allocentric Spatial Learning. *European Journal of Neuroscience, 2*(12), 1016-1028.
Moyer, J. R., Jr., Deyo, R. A., & Disterhoft, J. F. (1990). Hippocampectomy disrupts trace eye-blink conditioning in rabbits. *Behavioral Neuroscience, 104*(2), 243-252.
Mulle, C., Sailer, A., Perez-Otano, I., Dickinson-Anson, H., Castillo, P. E., Bureau, I., et al. (1998). Altered synaptic physiology and reduced susceptibility to kainate-induced seizures in GluR6-deficient mice. *Nature, 392*(6676), 601-605.
Napoli, C., Lemieux, C., & Jorgensen, R. (1990). Introduction of a Chimeric Chalcone Synthase Gene into Petunia Results in Reversible Co-Suppression of Homologous Genes in trans. *Plant Cell, 2*(4), 279-289.
Orr, W. B., & Berger, T. W. (1985). Hippocampectomy disrupts the topography of conditioned nictitating membrane responses during reversal learning. *Behavioral Neuroscience, 99*(1), 35-45.
Overstreet-Wadiche, L. S., Bensen, A. L., & Westbrook, G. L. (2006). Delayed development of adult-generated granule cells in dentate gyrus. *Journal of Neuroscience, 26*(8), 2326-2334.
Represa, A., Tremblay, E., & Ben-Ari, Y. (1987). Kainate binding sites in the hippocampal mossy fibers: localization and plasticity. *Neuroscience, 20*(3), 739-748.
Ribak, C. E., Seress, L., & Amaral, D. G. (1985). The development, ultrastructure and synaptic connections of the mossy cells of the dentate gyrus. *Journal of Neurocytology, 14*(5), 835-857.

Romano, N., & Macino, G. (1992). Quelling: transient inactivation of gene expression in Neurospora crassa by transformation with homologous sequences. *Molecular Microbiology, 6*(22), 3343-3353.
Schiffer, H. H., Swanson, G. T., & Heinemann, S. F. (1997). Rat GluR7 and a carboxy-terminal splice variant, GluR7b, are functional kainate receptor subunits with a low sensitivity to glutamate. *Neuron, 19*(5), 1141-1146.
Schmitz, D., Mellor, J., Breustedt, J., & Nicoll, R. A. (2003). Presynaptic kainate receptors impart an associative property to hippocampal mossy fiber long-term potentiation. *Nature Neuroscience, 6*(10), 1058-1063.
Schmitz, D., Mellor, J., Frerking, M., & Nicoll, R. A. (2001). Presynaptic kainate receptors at hippocampal mossy fiber synapses. *Proceedings of the National Academy of Sciences of the United States of America, 98*(20), 11003-11008.
Schmitz, D., Mellor, J., & Nicoll, R. A. (2001). Presynaptic kainate receptor mediation of frequency facilitation at hippocampal mossy fiber synapses. *Science, 291*(5510), 1972-1976.
Scoville, W. B., & Milner, B. (1957). Loss of recent memory after bilateral hippocampal lesions. *Journal of Neurology, Neurosurgery and Psychiatry, 20*(1), 11-21.
Seress, L. (1978). Pyramid-like basket cells in the granular layer of the dentate gyrus in the rat. *Journal of Anatomy, 127*(Pt 1), 163-168.
Shimomura, O., Johnson, F. H., & Saiga, Y. (1962). Extraction, purification and properties of aequorin, a bioluminescent protein from the luminous hydromedusan, Aequorea. *J Cell Comp Physiol, 59*, 223-239.
Shors, T. J., Miesegaes, G., Beylin, A., Zhao, M., Rydel, T., & Gould, E. (2001). Neurogenesis in the adult is involved in the formation of trace memories. *Nature, 410*(6826), 372-376.
Singer, B. H., Jutkiewicz, E. M., Fuller, C. L., Lichtenwalner, R. J., Zhang, H., Velander, A. J., et al. (2009). Conditional ablation and recovery of forebrain neurogenesis in the mouse. *Journal of Comparative Neurology, 514*(6), 567-582.
Snyder, J. S., Hong, N. S., McDonald, R. J., & Wojtowicz, J. M. (2005). A role for adult neurogenesis in spatial long-term memory. *Neuroscience, 130*(4), 843-852.
Snyder, J. S., Kee, N., & Wojtowicz, J. M. (2001). Effects of adult neurogenesis on synaptic plasticity in the rat dentate gyrus. *Journal of Neurophysiology, 85*(6), 2423-2431.
Sommer, B., Burnashev, N., Verdoorn, T. A., Keinanen, K., Sakmann, B., & Seeburg, P. H. (1992). A glutamate receptor channel with high affinity for domoate and kainate. *EMBO Journal, 11*(4), 1651-1656.
Squire, L. R., Stark, C. E., & Clark, R. E. (2004). The medial temporal lobe. *Annual Review of Neuroscience, 27*, 279-306.
Tashiro, A., Dunaevsky, A., Blazeski, R., Mason, C. A., & Yuste, R. (2003). Bidirectional regulation of hippocampal mossy fiber filopodial motility by kainate receptors: a two-step model of synaptogenesis. *Neuron, 38*(5), 773-784.
Tashiro, A., Makino, H., & Gage, F. H. (2007). Experience-specific functional modification of the dentate gyrus through adult neurogenesis: a critical period during an immature stage. *Journal of Neuroscience, 27*(12), 3252-3259.
Tronel, S., Fabre, A., Charrier, V., Oliet, S. H., Gage, F. H., & Abrous, D. N. (2010). Spatial learning sculpts the dendritic arbor of adult-born hippocampal neurons. *Proceedings of the National Academy of Sciences of the United States of America, 107*(17), 7963-7968.
van Praag, H., Christie, B. R., Sejnowski, T. J., & Gage, F. H. (1999). Running enhances neurogenesis, learning, and long-term potentiation in mice. *Proceedings of the National Academy of Sciences of the United States of America, 96*(23), 13427-13431.
Werner, P., Voigt, M., Keinanen, K., Wisden, W., & Seeburg, P. H. (1991). Cloning of a putative high-affinity kainate receptor expressed predominantly in hippocampal CA3 cells. *Nature, 351*(6329), 742-744.
Wisden, W., & Seeburg, P. H. (1993). A complex mosaic of high-affinity kainate receptors in rat brain. *Journal of Neuroscience, 13*(8), 3582-3598.

Wu, M. T., Wu, R. H., Hung, C. F., Cheng, T. L., Tsai, W. H., & Chang, W. T. (2005). Simple and efficient DNA vector-based RNAi systems in mammalian cells. *Biochemical and Biophysical Research Communications, 330*(1), 53-59.

Yu, J. Y., DeRuiter, S. L., & Turner, D. L. (2002). RNA interference by expression of short-interfering RNAs and hairpin RNAs in mammalian cells. *Proceedings of the National Academy of Sciences of the United States of America, 99*(9), 6047-6052.

Zeng, Y., Wagner, E. J., & Cullen, B. R. (2002). Both natural and designed micro RNAs can inhibit the expression of cognate mRNAs when expressed in human cells. *Molecular Cell, 9*(6), 1327-1333.

Zhao, C., Teng, E. M., Summers, R. G., Jr., Ming, G. L., & Gage, F. H. (2006). Distinct morphological stages of dentate granule neuron maturation in the adult mouse hippocampus. *Journal of Neuroscience, 26*(1), 3-11.